

Group selection and shrinkage with application to sparse semiparametric modeling

Ryan Thompson* Farshid Vahid†

May 26, 2021

Abstract

Sparse regression and classification estimators capable of group selection have application to an assortment of statistical problems, from multitask learning to sparse additive modeling to hierarchical selection. This work introduces a class of group-sparse estimators that combine group subset selection with group lasso or ridge shrinkage. We develop an optimization framework for fitting the nonconvex regularization surface and present finite-sample error bounds for estimation of the regression function. Our methods and analyses accommodate the general setting where groups overlap. As an application of group selection, we study sparse semiparametric modeling, a procedure that allows the effect of each predictor to be zero, linear, or nonlinear. For this task, the new estimators improve across several metrics on synthetic data compared to alternatives. Finally, we demonstrate their efficacy in modeling supermarket foot traffic and economic recessions using many predictors. All of our proposals are made available in the scalable implementation `grpse1`.

1 Introduction

Group selection (structured selection) arises in connection with a myriad of statistical problems, e.g., multitask learning (Obozinski et al. 2006), sparse additive modeling (Ravikumar et al. 2009), and hierarchical selection (Lim and Hastie 2015). Even sparse linear modeling can involve structured selection, such as when a categorical predictor is represented as a sequence of dummy variables. In certain domains, groups may emerge naturally, e.g., disaggregates of the same macroeconomic series or genes of the same biological path. The prevalence of such problems motivates principled estimation procedures capable of encoding structure into the fitted models they produce.

Given response $\mathbf{y} = (y_1, \dots, y_n)^\top \in \mathbb{R}^n$, predictors $\mathbf{X} = (\mathbf{x}_1, \dots, \mathbf{x}_n)^\top \in \mathbb{R}^{n \times p}$, and nonoverlapping groups $\mathcal{G}_1, \dots, \mathcal{G}_g \subseteq \{1, \dots, p\}$, group lasso (Yuan and Lin 2006; Meier et al.

*Monash University, Email: ryan.thompson@monash.edu

†Monash University, Email: farshid.vahid@monash.edu

Keywords: Coordinate descent, group lasso, group subset selection, structured sparsity, variable selection

2008) solves:

$$\min_{\beta \in \mathbb{R}^p} \sum_{i=1}^n \ell(\mathbf{x}_i^\top \beta, y_i) + \sum_{k=1}^g \lambda_k \|\beta_k\|_2, \quad (1.1)$$

where $\beta_k \in \mathbb{R}^{p_k}$ are the coefficients indexed by \mathcal{G}_k , $\lambda_1, \dots, \lambda_g$ are nonnegative tuning parameters, and $\ell: \mathbb{R}^2 \rightarrow \mathbb{R}_+$ is a loss function, e.g., square loss for regression or logistic loss for classification.¹ Group lasso couples coefficients via their l_2 -norm so that all predictors in a group are selected together.

Just as lasso (Tibshirani 1996) is the continuous relaxation of the combinatorially-hard problem of best subset selection (“best subset”), so is group lasso the relaxation of the combinatorial problem of group subset selection (“group subset”):

$$\min_{\beta \in \mathbb{R}^p} \sum_{i=1}^n \ell(\mathbf{x}_i^\top \beta, y_i) + \sum_{k=1}^g \lambda_k 1(\|\beta_k\|_2 \neq 0). \quad (1.2)$$

Unlike group lasso, which promotes group sparsity implicitly by nondifferentiability of the l_2 -norm at the null vector, group subset explicitly penalizes the number of nonzero groups. Consequently, one might interpret group lasso as a compromise made in the interest of computation. However, group lasso has a trick up its sleeve that group subset does not: shrinkage. Shrinkage estimators such as lasso and ridge (Hoerl and Kennard 1970) are more robust than best subset to noise (Breiman 1996; Hastie et al. 2020). This consideration motivates us to shrink the group subset estimator:

$$\min_{\beta \in \mathbb{R}^p} \sum_{i=1}^n \ell(\mathbf{x}_i^\top \beta, y_i) + \sum_{k=1}^g \lambda_{0k} 1(\|\beta_k\|_2 \neq 0) + \sum_{k=1}^g \lambda_{qk} \|\beta_k\|_2^q, \quad q \in \{1, 2\}. \quad (1.3)$$

In contrast to group lasso and group subset, (1.3) directly controls both group sparsity and shrinkage via separate penalties. When $q = 1$, the shrinkage penalty is group lasso, and when $q = 2$, the penalty is ridge. The combination of best subset and lasso or ridge in the unstructured setting results in good predictive models with low false positive selection rates (Mazumder et al. 2020).

Unfortunately, the estimators (1.3), including group lasso and group subset as special cases, do not accommodate overlap among groups. Specifically, if two groups overlap, one cannot be selected independently of the other. To encode sophisticated structures, such as hierarchies or graphs, groups must often overlap. To address this issue, one can introduce group-specific vectors $\boldsymbol{\nu}^{(k)} \in \mathbb{R}^p$ ($k = 1, \dots, g$) that are zero everywhere except at the positions indexed by \mathcal{G}_k . Letting \mathcal{V} be the set of all tuples $\bar{\boldsymbol{\nu}} := (\boldsymbol{\nu}^{(1)}, \dots, \boldsymbol{\nu}^{(g)})$ satisfying this property, group subset with shrinkage becomes:

$$\min_{\substack{\beta \in \mathbb{R}^p, \bar{\boldsymbol{\nu}} \in \mathcal{V} \\ \beta = \sum_{k=1}^g \boldsymbol{\nu}^{(k)}}} \sum_{i=1}^n \ell(\mathbf{x}_i^\top \beta, y_i) + \sum_{k=1}^g \lambda_{0k} 1(\|\boldsymbol{\nu}^{(k)}\|_2 \neq 0) + \sum_{k=1}^g \lambda_{qk} \|\boldsymbol{\nu}^{(k)}\|_2^q, \quad q \in \{1, 2\}. \quad (1.4)$$

The vectors $\boldsymbol{\nu}^{(1)}, \dots, \boldsymbol{\nu}^{(g)}$ are a decomposition of β into a sum of latent coefficients that facilitate selection of overlapping groups. For instance, if three predictors, x_1 , x_2 , and x_3 , are

¹Here and throughout, the intercept term is omitted to facilitate exposition.

spread across two groups, $\mathcal{G}_1 = \{1, 2\}$ and $\mathcal{G}_2 = \{2, 3\}$, then $\beta_1 = \nu_1^{(1)}$, $\beta_2 = \nu_2^{(1)} + \nu_2^{(2)}$, and $\beta_3 = \nu_3^{(2)}$. Since β_2 has a separate latent coefficient for each group, \mathcal{G}_1 or \mathcal{G}_2 can be selected independently of the other. This latent coefficient approach originated for group lasso with Jacob et al. (2009) and Obozinski et al. (2011). When all groups are disjoint, (1.4) reduces exactly to (1.3).

This paper develops computational methods and statistical theory for group subset with shrinkage. Via the formulation (1.4), our work accommodates the general overlapping groups setting. On the computational side, we develop algorithms that scale to compute quality (approximate) solutions of the combinatorial optimization problem. Our framework comprises coordinate descent and local search and applies to general smooth convex loss functions (i.e., regression and classification), building on recent advances for best subset (Dedieu et al. 2020; Hazimeh and Mazumder 2020). In contrast to existing computational methods for group subset (Guo et al. 2014; Bertsimas and King 2016), which rely on branch-and-bound or commercial mixed-integer optimizers, our methods scale to instances with millions of predictors or groups. We implement our framework in the publicly available R package `grpssel`. On the statistical side, we establish new error bounds for group subset with and without shrinkage. The bounds apply in the overlapping setting and allow for model misspecification. The analysis sheds light on the advantages of group selection and the benefits of shrinkage.

The new estimators have application to a broad range of statistical problems. We focus on sparse semiparametric modeling, a procedure wherein y is modeled via a sum of functions $\sum_j f_j(x_j)$, and f_j can be zero, linear, or nonlinear. Chouldechova and Hastie (2015) and Lou et al. (2016) estimate these flexible models using group lasso with overlapping groups and regression splines. After conducting synthetic experiments on the efficacy of our estimators in fitting these models, we carry out two empirical studies. The first study involves modeling supermarket foot traffic using sales volumes on different products. Only a fraction of supermarket products are traded in volume, necessitating sparsity. The second study involves modeling recessionary periods in the economy using macroeconomic series. The macroeconomic literature contains many examples of sparse linear modeling (De Mol et al. 2008; Li and Chen 2014), yet theory does not dictate linearity. Together these studies suggest semiparametric models are an excellent compromise between fully linear and fully nonparametric alternatives.

Independently and concurrently to this work, Hazimeh et al. (2021) study computation and theory for group subset with nonoverlapping groups. Their algorithms likewise build on Hazimeh and Mazumder (2020) but apply only to square loss regression. In another recent preprint, Zhang et al. (2021) propose a computational “splicing” technique for group subset that appears promising, though they do not consider overlapping groups or shrinkage.

The paper is structured as follows. Section 2 presents computational methods, Section 3 provides statistical theory, Section 4 describes simulation experiments, Section 5 reports data analyses, and Section 6 closes the paper. All proofs are relegated to the appendices.

2 Computation

This section introduces our optimization framework and its key components: coordinate descent and local search. The framework applies to any smooth convex loss function $\ell(z, y)$.

The discussion below addresses the specific cases of square loss $\ell(z, y) = (y - z)^2/2$, which is suitable for regression, and logistic loss $\ell(z, y) = -y \log(z) - (1 - y) \log(1 - z)$, which is suitable for classification. Both loss functions are implemented in `grpse1`.

The algorithms are presented for nonoverlapping groups; however, this does not limit their applicability since the overlapping groups problem can be transformed into one involving disjoint groups. Let $\tilde{\mathbf{X}} := (\mathbf{X}_1, \dots, \mathbf{X}_g)$ be the predictor matrix formed by concatenating the submatrices of \mathbf{X} corresponding to groups $\mathcal{G}_1, \dots, \mathcal{G}_g$. Since the predictors are replicated as many times as they appear across groups, a new set of groups that do not overlap can be constructed. The algorithms are then run on $\tilde{\mathbf{X}}$ with the new groups. Finally, the coefficients on \mathbf{X} are recovered by summing the coefficients on each replicated column in $\tilde{\mathbf{X}}$. Jacob et al. (2009) suggest this approach for group lasso. The matrix $\tilde{\mathbf{X}}$, however, will not be full rank, nor will a submatrix corresponding to any subset of overlapping groups. Our algorithmic analysis takes this fact into account.

Throughout this section, \mathbf{X} is assumed to have columns with mean zero and unit l_2 -norm.

2.1 Coordinate descent

Coordinate descent algorithms are optimization routines that minimize along successive coordinate hyperplanes. The coordinate descent scheme developed here iteratively fixes all but one group of coordinates (a coordinate group) and minimizes in the directions of these coordinates.

The group subset problem (1.4) can be expressed as the unconstrained minimizer of the objective function $F(\boldsymbol{\beta}) := L(\boldsymbol{\beta}) + \Omega(\boldsymbol{\beta})$, where the loss function

$$L(\boldsymbol{\beta}) := \sum_{i=1}^n \ell(\mathbf{x}_i^\top \boldsymbol{\beta}, y_i),$$

and the regularization function

$$\Omega(\boldsymbol{\beta}) := \sum_{k=1}^g (\lambda_{0k} 1(\|\boldsymbol{\beta}_k\|_2 \neq 0) + \lambda_{1k} \|\boldsymbol{\beta}_k\|_2 + \lambda_{2k} \|\boldsymbol{\beta}_k\|_2^2).$$

The regularization function can be written directly in terms of $\boldsymbol{\beta}_k$ since the groups are transformed such that they do not overlap. The function $F(\boldsymbol{\beta})$ is a sum of smooth convex and discontinuous nonconvex functions and is hence discontinuous nonconvex. The minimization problem with respect to group k is

$$\min_{\boldsymbol{\xi} \in \mathbb{R}^{p_k}} F(\boldsymbol{\beta}_1, \dots, \boldsymbol{\beta}_{k-1}, \boldsymbol{\xi}, \boldsymbol{\beta}_{k+1}, \dots, \boldsymbol{\beta}_g). \quad (2.1)$$

The complexity of this coordinate-wise minimization depends on ℓ and \mathbf{X} . In the case of square loss, the minimization involves a least-squares fit in p_k coordinates, taking $O(p_k^2 n)$ operations. To bypass these involved computations, a partial minimization scheme is adopted whereby each coordinate group is updated using a single gradient descent step taken with respect to that group. This scheme results from a standard technique of replacing the objective function with a surrogate function that is a quadratic upper bound. To this end, we require Lemma 2.1.

Lemma 2.1. *Let $L : \mathbb{R}^p \rightarrow \mathbb{R}$ be a continuously differentiable function. Suppose there exists a $c_k > 0$ such that the gradient of L with respect to group k satisfies the Lipschitz property*

$$\|\nabla_k L(\boldsymbol{\beta}) - \nabla_k L(\tilde{\boldsymbol{\beta}})\|_2 \leq c_k \|\boldsymbol{\beta}_k - \tilde{\boldsymbol{\beta}}_k\|_2,$$

for all $\boldsymbol{\beta} \in \mathbb{R}^p$ and $\tilde{\boldsymbol{\beta}} \in \mathbb{R}^p$ that differ only in group k . Then it holds

$$L(\boldsymbol{\beta}) \leq \bar{L}_{\bar{c}_k}(\boldsymbol{\beta}; \tilde{\boldsymbol{\beta}}) := L(\tilde{\boldsymbol{\beta}}) + \nabla_k L(\tilde{\boldsymbol{\beta}})^\top (\boldsymbol{\beta}_k - \tilde{\boldsymbol{\beta}}_k) + \frac{\bar{c}_k}{2} \|\boldsymbol{\beta}_k - \tilde{\boldsymbol{\beta}}_k\|_2^2, \quad (2.2)$$

for any $\bar{c}_k \geq c_k$.

Lemma 2.1 is the block descent lemma of Beck and Tetrushvili (2013), which holds under a Lipschitz condition on the group-wise gradients of $L(\boldsymbol{\beta})$. This condition is satisfied for square loss with $c_k = \gamma_k^2$ and for logistic loss with $c_k = \gamma_k^2/4$, where γ_k is the maximal eigenvalue of $\mathbf{X}_k^\top \mathbf{X}_k$. Using the result of Lemma 2.1, a quadratic upper bound of $F(\boldsymbol{\beta})$, treated as a function in group k , is given by

$$\bar{F}_{\bar{c}_k}(\boldsymbol{\beta}; \tilde{\boldsymbol{\beta}}) := \bar{L}_{\bar{c}_k}(\boldsymbol{\beta}; \tilde{\boldsymbol{\beta}}) + \Omega(\boldsymbol{\beta}). \quad (2.3)$$

Thus, in place of the minimization (2.1), we use the minimization

$$\min_{\boldsymbol{\xi} \in \mathbb{R}^{p_k}} \bar{F}_{\bar{c}_k}(\boldsymbol{\beta}_1, \dots, \boldsymbol{\beta}_{k-1}, \boldsymbol{\xi}, \boldsymbol{\beta}_{k+1}, \dots, \boldsymbol{\beta}_g; \tilde{\boldsymbol{\beta}}). \quad (2.4)$$

This new problem admits a simple analytical solution, given by Proposition 2.1.

Proposition 2.1. *Define the thresholding function*

$$T_c(\boldsymbol{\beta}; \lambda_0, \lambda_1, \lambda_2) := \begin{cases} \phi \boldsymbol{\beta} & \text{if } \phi \|\boldsymbol{\beta}\|_2 \geq \sqrt{\frac{2\lambda_0}{c + 2\lambda_2}} \\ \mathbf{0} & \text{otherwise,} \end{cases} \quad (2.5)$$

where

$$\phi = \frac{c}{c + 2\lambda_2} \left(1 - \frac{\lambda_1}{c \|\boldsymbol{\beta}\|_2} \right)_+$$

and $(x)_+$ is shorthand for $\max(x, 0)$. Then the coordinate-wise minimization problem (2.4) is solved by

$$\boldsymbol{\beta}_k^* = T_{\bar{c}_k} \left(\tilde{\boldsymbol{\beta}}_k - \frac{1}{\bar{c}_k} \nabla_k L(\tilde{\boldsymbol{\beta}}); \lambda_{0k}, \lambda_{1k}, \lambda_{2k} \right).$$

Proposition 2.1 states that a minimizer is given by appropriately thresholding a gradient descent update to coordinate group k . For both square and logistic loss, the gradient $\nabla_k L(\tilde{\boldsymbol{\beta}})$ can be expressed as

$$\nabla_k L(\tilde{\boldsymbol{\beta}}) = -\mathbf{X}_k^\top \mathbf{r},$$

where $\mathbf{r} = \mathbf{y} - \mathbf{X}\tilde{\boldsymbol{\beta}}$ for square loss and $\mathbf{r} = \mathbf{y} - (1 + \exp(-\mathbf{X}\tilde{\boldsymbol{\beta}}))^{-1}$ for logistic loss. Hence, a solution to (2.4) can be computed in as few as $O(p_k n)$ operations.

Algorithm 1 now presents the coordinate descent scheme. Several algorithmic optimizations and heuristics can improve performance; these are discussed in Section 2.3.

Algorithm 1: Coordinate descent

```
input :  $\beta^{(0)} \in \mathbb{R}^p$ 
for  $m = 1, 2, \dots$  do
     $\beta^{(m)} \leftarrow \beta^{(m-1)}$ 
    for  $k = 1, \dots, g$  do
         $\beta_k^{(m)} \leftarrow \arg \min_{\xi \in \mathbb{R}^{p_k}} \bar{F}_{\bar{c}_k}(\beta_1^{(m)}, \dots, \beta_{k-1}^{(m)}, \xi, \beta_{k+1}^{(m)}, \dots, \beta_g^{(m)}; \beta^{(m)})$ 
    end
    if converged then break
end
return  $\beta^{(m)}$ 
```

2.1.1 Convergence analysis

While Algorithm 1 may appear as an otherwise standard coordinate descent algorithm, the presence of the group subset penalty complicates the analysis of its convergence properties. No standard convergence results directly apply; e.g., Tseng (2001) that applies to group lasso cannot be invoked immediately here. Hence, we work towards establishing some properties tailored to Algorithm 1.

Two results are presented. Lemma 2.2 establishes convergence of the sequence of objective values. Theorem 2.1 establishes convergence of the sequence of iterates to a stationary point of $F(\beta)$ that satisfies a certain coordinate-wise property. A point β^* with nonzero coordinate groups \mathcal{A}^* is said to be a stationary point of $F(\beta)$ if $\nabla_{\mathcal{A}^*} L(\beta^*) = \mathbf{0}$.

Lemma 2.2. *Let $\bar{c}_k \geq c_k$ for all $k = 1, \dots, g$. Then the sequence of objective values $\{F(\beta^{(m)})\}_{m \in \mathbb{N}}$ produced by Algorithm 1 is decreasing, convergent, and satisfies the inequality*

$$F(\beta^{(m)}) - F(\beta^{(m+1)}) \geq \sum_{k=1}^g \frac{\bar{c}_k - c_k}{2} \|\beta_k^{(m+1)} - \beta_k^{(m)}\|_2^2.$$

Lemma 2.2 is derived from the result of Lemma 2.1.

Theorem 2.1. *Let $\bar{c}_k > c_k$ for all $k = 1, \dots, g$. Then the sequence of iterates $\{\beta^{(m)}\}_{m \in \mathbb{N}}$ produced by Algorithm 1 converge to a solution β^* that is a stationary point of $F(\beta)$ satisfying the fixed point equations*

$$\beta_k^* = T_{\bar{c}_k} \left(\beta_k^* - \frac{1}{\bar{c}_k} \nabla_k L(\beta^*); \lambda_{0k}, \lambda_{1k}, \lambda_{2k} \right), \quad k = 1, \dots, g. \quad (2.6)$$

To prove Theorem 2.1, Lemma 2.2 is used to show that the active set stabilizes during coordinate descent. This property allows the group subset penalty to be treated as a fixed quantity after some finite number of iterations, and in turn, opens up the results of Tseng (2001).

The fixed point equations in Theorem 2.1 have the interpretation that the limit point of the iterates of Algorithm 1 cannot be improved by partially minimizing in the directions

of any coordinate group. This notion is stronger than stationarity alone because all points satisfying (2.6) are stationary, but not all stationary points satisfy (2.6).

In the case of overlapping groups, the matrix $\tilde{\mathbf{X}} := (\mathbf{X}_1, \dots, \mathbf{X}_g)$ is rank deficient, as are any of its submatrices corresponding to groups that overlap. This matter raises a question as to whether the convergence results established above still hold. As summarized in the following remark, the answer is in the affirmative.

Remark 2.1. *Let $\mathcal{G}_1, \dots, \mathcal{G}_g$ be a set of overlapping groups. Then Theorem 2.1 remains valid when Algorithm 1 is run with the predictor matrix $\tilde{\mathbf{X}} := (\mathbf{X}_1, \dots, \mathbf{X}_g)$, where \mathbf{X}_k contains the columns of \mathbf{X} indexed by \mathcal{G}_k .*

This claim follows from an inspection of the relevant proofs.

2.2 Local search

Local search methods have a long history in combinatorial optimization. Here we present a local search method tailored specifically to the group subset problem. The proposed method generalizes an algorithm that first appeared in Beck and Eldar (2013) for solving instances of unstructured sparse optimization. Hazimeh and Mazumder (2020) and Dedieu et al. (2020) adapt it to best subset with promising results. The core idea is simple: given an incumbent solution, search a neighborhood local to that solution for a minimizer with lower objective value by discretely optimizing over a small set of coordinate groups. This scheme turns out to be useful when the predictors are strongly correlated, a situation in which coordinate descent alone may produce a poor solution.

Define the group sparsity pattern of a vector β to be the set of nonzero group indices:²

$$\text{gs}(\beta) := \{k \in \{1, \dots, g\} : \|\beta_k\|_2 \neq 0\},$$

and define the constraints sets

$$C_s^1(\beta) := \left\{ \mathbf{e} \in \{0, 1\}^p : \text{gs}(\mathbf{e}) \subseteq \text{gs}(\beta), \sum_{k=1}^g 1(\|\mathbf{e}_k\|_2 \neq 0) \leq s \right\}$$

and

$$C_s^2(\beta) := \left\{ \mathbf{e} \in \{0, 1\}^p : \text{gs}(\mathbf{e}) \not\subseteq \text{gs}(\beta), \sum_{k=1}^g 1(\|\mathbf{e}_k\|_2 \neq 0) \leq s \right\}.$$

Now, consider the optimization problem

$$\min_{\xi \in \mathbb{R}^p, \mathbf{e}^1 \in C_s^1(\beta), \mathbf{e}^2 \in C_s^2(\beta)} F(\beta - \mathbf{e}^1 \beta + \mathbf{e}^2 \xi). \quad (2.7)$$

Given a fixed vector β , a solution to (2.7) is a minimizer among all ways of replacing a subset of active coordinate groups in β with a new subset. The complexity of the problem is dictated by s , which controls the size of these subsets. When $s = g$, the full combinatorial problem whose solution is a global minimizer of the group subset problem is recovered. For $s \ll g$, a reduced combinatorial problem is obtained whose solution space is usually orders of magnitude smaller than that of the full problem.

Algorithm 2: Local search

```
input :  $\beta \in \mathbb{R}^p$ 
 $\mathcal{A} \leftarrow \text{gs}(\beta)$ 
for  $k \in \mathcal{A}$  do
  for  $j \notin \mathcal{A}$  do
     $\beta^{(j)} \leftarrow \beta$ 
     $\beta_k^{(j)} \leftarrow \mathbf{0}$ 
     $\beta_j^{(j)} \leftarrow \arg \min_{\xi \in \mathbb{R}^{p_j}} F(\beta_1^{(j)}, \dots, \beta_{j-1}^{(j)}, \xi, \beta_{j+1}^{(j)}, \dots, \beta_g^{(j)})$ 
  end
   $j^* \leftarrow \arg \min_{j \notin \mathcal{A}} F(\beta^{(j)})$ 
  if  $F(\beta^{(j^*)}) < F(\beta)$  then
     $\beta \leftarrow \beta^{(j^*)}$ 
    break
  end
end
return  $\beta$ 
```

The limiting case $s = 1$ admits an efficient computational scheme, given in Algorithm 2, referred to hereafter as local search. Algorithm 2 comprises two low-complexity loops: an outer loop over the active set and an inner loop over the inactive set. Within the inner loop, an active coordinate group is removed, and the objective is minimized in the directions of an inactive coordinate group. This minimization problem can be solved by iterating the thresholding operator (2.5).

Since Algorithm 2 involves optimizing in one coordinate group only, it need not produce a stationary point even if initialized at one. Algorithm 3 thus combines local search with coordinate descent. The combined algorithm first produces a candidate solution using

Algorithm 3: Coordinate descent with local search

```
input :  $\beta^{(0)} \in \mathbb{R}^p$ 
for  $m = 1, 2, \dots$  do
   $\beta^{(m)} \leftarrow$  output of Algorithm 1 initialized with  $\beta^{(m-1)}$ 
   $\tilde{\beta}^{(m)} \leftarrow$  output of Algorithm 2 initialized with  $\beta^{(m)}$ 
  if  $\beta^{(m)} = \tilde{\beta}^{(m)}$  then break
end
return  $\beta^{(m)}$ 
```

coordinate descent and then follows up with local search. This scheme is iterated until the solution cannot be improved. Compared with coordinate descent alone, coordinate descent with local search can yield significantly lower objective values in high-correlation

²Recall the groups have been transformed such that they do not overlap; hence, $\text{gs}(\beta)$ is well-defined.

scenarios. Empirical comparisons of the algorithms are provided in Section 4. Algorithm 3 is guaranteed to converge because Algorithm 2 never increases the objective value (by construction), Algorithm 1 is convergent, and the objective function is bounded below.

2.3 Other components

This section is concluded with details of additional components of the framework. Some components are described in Appendix A.5 in the interest of space.

2.3.1 Orthogonal groups

Suppose the group matrix \mathbf{X}_k is orthogonal, i.e., $\mathbf{X}_k^\top \mathbf{X}_k = \mathbf{I}$. Then, for square loss, the surrogate minimization problem (2.4) *exactly* minimizes $F(\boldsymbol{\beta})$ with respect to group k when $\bar{c}_k = c_k$. If the groups are not orthogonal, they can be made so using singular value decomposition. The coefficients can then be transformed back to their original basis after the algorithms have run. Experimental evidence suggests orthogonal groups yield higher quality solutions in fewer iterations. In addition, using orthogonal groups is equivalent to using the regularizer $\Omega(\mathbf{X}\boldsymbol{\beta})$. That is, orthogonalizing the groups has the effect of penalizing the fits $\mathbf{X}_k\boldsymbol{\beta}_k$ rather than the coefficients $\boldsymbol{\beta}_k$. For many problems, this type of penalization is intuitive; e.g., when \mathbf{X}_k represents a basis for a function f_k , penalizing $\mathbf{X}_k\boldsymbol{\beta}_k$ is equivalent to penalizing the complexity of f_k . Simon and Tibshirani (2012) point out this property for group lasso. Our implementation supports automatic orthogonalization.

2.3.2 Regularization parameters

To ensure equitable penalization among possibly unequally sized groups, the parameters λ_{0k} and λ_{qk} are configured to reflect the group size p_k . Suitable default choices are $\lambda_{0k} = p_k \lambda_0$, $\lambda_{1k} = \sqrt{p_k} \lambda_1$, and $\lambda_{2k} = \lambda_2$, where λ_0 , λ_1 , and λ_2 are nonnegative. The ridge parameter λ_{2k} is typically fixed across k since the ridge penalty decouples the groupings.³ For fixed λ_q , we take a sequence $\{\lambda_0^{(t)}\}_{t=1}^T$ such that $\lambda_0^{(0)}$ yields $\hat{\boldsymbol{\beta}} = \mathbf{0}$, and sequentially warm start the algorithms. That is, the solution for $\lambda_0^{(t+1)}$ is obtained by using the solution from $\lambda_0^{(t)}$ as an initialization point. The sequence $\{\lambda_0^{(t)}\}_{t=1}^T$ is computed in such a way that the active set of groups corresponding to $\lambda_0^{(t+1)}$ is always different to that corresponding to $\lambda_0^{(t)}$. Proposition 2.2 presents the details of this method, extending an idea of Hazimeh and Mazumder (2020) for best subset.

Proposition 2.2. *Suppose that $\hat{\boldsymbol{\beta}}^{(t)}$ is the result of running Algorithm 1 with $\lambda_0 = \lambda_0^{(t)}$. Let $\mathcal{A}^{(t)}$ be the active set of groups. Then running Algorithm 1 initialized to $\hat{\boldsymbol{\beta}}^{(t)}$ and using $\lambda_0 = \lambda_0^{(t+1)}$ where*

$$\lambda_0^{(t+1)} = \alpha \cdot \max_{k \notin \mathcal{A}^{(t)}} \left(\frac{\left(\|\nabla L(\hat{\boldsymbol{\beta}}^{(t)})\|_2 - \lambda_{1k} \right)_+^2}{2p_k(\bar{c}_k + 2\lambda_{2k})} \right)$$

produces a solution $\hat{\boldsymbol{\beta}}^{(t+1)}$ such that $\hat{\boldsymbol{\beta}}^{(t+1)} \neq \hat{\boldsymbol{\beta}}^{(t)}$ for any $\alpha \in [0, 1)$.

³The decoupling occurs because $\sum_{k=1}^g \|\boldsymbol{\beta}_k\|_2^2 = \|\boldsymbol{\beta}\|_2^2$.

3 Error bounds

This section presents a finite-sample analysis of the proposed estimators. In particular, we state probabilistic upper bounds for the error of estimating the underlying regression function. These bounds accommodate overlapping groups and model misspecification. The role of structure and shrinkage is discussed, and comparisons are made with known bounds for other estimators.

3.1 Setup

The data is assumed to be generated according to the regression model

$$y_i = f^0(\mathbf{x}_i) + \varepsilon_i, \quad i = 1, \dots, n,$$

where $f^0 : \mathbb{R}^p \rightarrow \mathbb{R}$ is a regression function, $\mathbf{x}_i \in \mathbb{R}^p$ are fixed predictors, and $\varepsilon_i \sim \mathcal{N}(0, \sigma^2)$ is iid stochastic noise. This flexible specification encompasses the semiparametric model $f^0(\mathbf{x}) = \sum_j f_j(x_j)$ (with f_j zero, linear, or nonlinear) that is the focus of our empirical studies, and the linear model $f^0(\mathbf{x}) = \mathbf{x}^\top \boldsymbol{\beta}^0$. Let $\mathbf{f}^0 := (f^0(\mathbf{x}_1), \dots, f^0(\mathbf{x}_n))^\top$ be the vector of function evaluations at the sample points. The goal of this section is to place probabilistic upper bounds on $\|\mathbf{f}^0 - \hat{\mathbf{f}}\|_2^2/n$, the estimation error of $\hat{\mathbf{f}} := \mathbf{X}\hat{\boldsymbol{\beta}}$.

The objects of our analysis are the group subset estimators (1.4). We allow the predictor groups $\mathcal{G}_1, \dots, \mathcal{G}_g$ to overlap, and do not require the group matrices $\mathbf{X}_1, \dots, \mathbf{X}_g$ to be orthogonal. To simplify the results and their derivations, we constrain the number of nonzero groups rather than penalize them. To this end, let $\mathcal{V}(s)$ be the set of all $\boldsymbol{\nu}$ such that at most s groups are nonzero:⁴

$$\mathcal{V}(s) := \left\{ \boldsymbol{\nu} \in \mathcal{V} : \sum_{k=1}^g 1(\|\boldsymbol{\nu}^{(k)}\|_2 \neq 0) \leq s \right\}.$$

We consider the regular group subset estimator:

$$\min_{\substack{\boldsymbol{\beta} \in \mathbb{R}^p, \boldsymbol{\nu} \in \mathcal{V}(s) \\ \boldsymbol{\beta} = \sum_{k=1}^g \boldsymbol{\nu}^{(k)}}} \frac{1}{n} \|\mathbf{y} - \mathbf{X}\boldsymbol{\beta}\|_2^2, \quad (3.1)$$

and the shrinkage estimator:

$$\min_{\substack{\boldsymbol{\beta} \in \mathbb{R}^p, \boldsymbol{\nu} \in \mathcal{V}(s) \\ \boldsymbol{\beta} = \sum_{k=1}^g \boldsymbol{\nu}^{(k)}}} \frac{1}{n} \|\mathbf{y} - \mathbf{X}\boldsymbol{\beta}\|_2^2 + 2 \sum_{k=1}^g \lambda_k \|\boldsymbol{\nu}^{(k)}\|_2^q. \quad (3.2)$$

The analysis focuses on the case $q = 1$ of group lasso shrinkage.

The results derived below apply to global minimizers of these nonconvex problems. The algorithms of the preceding section cannot guarantee such minimizers in general, but experiments in the subsequent section demonstrate they frequently attain them. If global

⁴For all values of the group subset penalty parameter λ_0 , there exists a constraint parameter s which yields an identical solution.

optimality is of foremost concern, the output of the algorithms can be used to initialize a mixed-integer optimizer (see Appendix C.1) which can guarantee a global solution at additional computational expense. In recent work, Fan et al. (2020) show that statistical properties of best subset remain valid when the attained minimum is within a neighborhood of the global minimum. We expect their analysis extends to structured settings.

3.2 Bound for group subset

We begin with Theorem 3.1, which characterizes an upper bound for group subset with no shrinkage. The notation $p_{\max} := \max_k p_k$ represents the maximal group size. As is customary, we absorb numerical constants into the term $C > 0$.

Theorem 3.1. *Let $\delta \in (0, 1]$ and $\alpha \in (0, 1)$. Then, for some numerical constant $C > 0$, the group subset estimator (3.1) satisfies*

$$\frac{1}{n} \|\mathbf{f}^0 - \hat{\mathbf{f}}\|_2^2 \leq \min_{\substack{\boldsymbol{\beta} \in \mathbb{R}^p, \boldsymbol{\nu} \in \mathcal{V}(s) \\ \boldsymbol{\beta} = \sum_{k=1}^g \boldsymbol{\nu}^{(k)}}} \frac{1 + \alpha}{(1 - \alpha)n} \|\mathbf{f}^0 - \mathbf{X}\boldsymbol{\beta}\|_2^2 + \frac{C\sigma^2}{\alpha(1 - \alpha)n} \left[sp_{\max} + s \log\left(\frac{g}{s}\right) + \log(\delta^{-1}) \right] \quad (3.3)$$

with probability at least $1 - \delta$.

The first term on the right-hand side of (3.3) is the error incurred by the oracle in approximating \mathbf{f}^0 as $\mathbf{X}\boldsymbol{\beta}$. In general, this error is unavoidable in finite-dimensional settings. The three terms inside the brackets have the following interpretations. The first term is the cost of estimating $\boldsymbol{\beta}$; with s active groups, there are at most $s \times p_{\max}$ parameters to estimate. The second term is the price of selection; it follows from an upper bound on the total number of group subsets. The third term controls the trade-off between the tightness of the bound and the probability it is satisfied. Finally, the scalar α appears in the bound due to the proof technique (as in, e.g., Rigollet 2015). When $\mathbf{f}^0 = \mathbf{X}\boldsymbol{\beta}^0$, α need not appear. Hazimeh et al. (2021) independently state an analogous bound for $\mathbf{f}^0 = \mathbf{X}\boldsymbol{\beta}^0$ in the case of equisized nonoverlapping groups. In the special case that all groups singletons, (3.3) matches the well-known bound for best subset (Raskutti et al. 2011).

Theorem 3.1 confirms group subset is preferable to best subset in structured settings. Consider the following example. Suppose we have g groups each of size p_0 so that the total number of predictors is $p = g \times p_0$. It follows for group sparsity level s that the ungrouped selection problem involves choosing $s \times p_0$ predictors. Accordingly, the ungrouped bound scales as $sp_0 + sp_0 \log(p/(sp_0)) = sp_0 + sp_0 \log(g/s)$. On the other hand, the grouped bound scales as $sp_0 + s \log(g/s)$, i.e., it improves by a factor p_0 of the logarithm term.

3.3 Bounds for group subset with shrinkage

We now establish bounds for group subset with shrinkage. The results are analogous to those established in Mazumder et al. (2020) for best subset with shrinkage. Two results are given, a bound where the error decays as $1/\sqrt{n}$, and another where the error decays as $1/n$. Adopting standard terminology (e.g., Hastie et al. 2015), the former bound is referred to as a “slow rate” and the latter bound as a “fast rate.”

The slow rate is presented in Theorem 3.2.

Theorem 3.2. Let $\delta \in (0, 1]$. Let γ_k be the maximal eigenvalue of the matrix $\mathbf{X}_k^\top \mathbf{X}_k / n$ and

$$\lambda_k \geq \frac{\sqrt{\gamma_k} \sigma}{\sqrt{n}} \sqrt{p_k + 2\sqrt{p_k \log(g) + p_k \log(\delta^{-1})} + 2\log(g) + 2\log(\delta^{-1})}, \quad k = 1, \dots, g.$$

Then the group subset estimator (3.2) with $q = 1$ satisfies

$$\frac{1}{n} \|\mathbf{f}^0 - \hat{\mathbf{f}}\|_2^2 \leq \min_{\substack{\boldsymbol{\beta} \in \mathbb{R}^p, \bar{\boldsymbol{\nu}} \in \mathcal{V}(s) \\ \boldsymbol{\beta} = \sum_{k=1}^g \boldsymbol{\nu}^{(k)}}} \frac{1}{n} \|\mathbf{f}^0 - \mathbf{X}\boldsymbol{\beta}\|_2^2 + 4 \sum_{k=1}^g \lambda_k \|\boldsymbol{\nu}^{(k)}\|_2 \quad (3.4)$$

with probability at least $1 - \delta$.

In the case of no overlap, Theorem 3.2 demonstrates that the shrinkage estimator satisfies the same slow rate as group lasso (Lounici et al. 2011, Theorem 3.1). An identical expression to Lounici et al. (2011) for λ_k can be stated here using a more intricate chi-squared tail bound in the proof. In the case of overlap, the same slow rate can be obtained for group lasso from Percival (2012, Lemma 4).

The following assumption is required to establish the fast rate.

Assumption 3.1. Let $s < \min(n/p_{\max}, g)/2$. Then there exists a $\phi(2s) > 0$ such that

$$\min_{\substack{\boldsymbol{\theta} \in \mathbb{R}^p, \bar{\boldsymbol{\nu}} \in \mathcal{V}(2s) \\ \boldsymbol{\theta} = \sum_{k=1}^g \boldsymbol{\nu}^{(k)} \neq \mathbf{0}}} \frac{\|\mathbf{X}\boldsymbol{\theta}\|_2}{\sqrt{n} \sum_{k=1}^g \|\boldsymbol{\nu}^{(k)}\|_2} \geq \phi(2s).$$

Assumption 3.1 is satisfied provided no collection of $2s$ groups have linearly dependent columns in \mathbf{X} . This condition is a weaker version of the restricted eigenvalue condition used in Lounici et al. (2011) and Percival (2012) for group lasso, which (loosely speaking) places additional restrictions on the correlations of the columns in \mathbf{X} .

The fast rate is presented in Theorem 3.3. The notation $\lambda_{\max} := \max_k \lambda_k$ represents the maximal shrinkage parameter.

Theorem 3.3. Let Assumption 3.1 hold. Let $\delta \in (0, 1]$ and $\alpha \in (0, 1)$. Let $\lambda_1, \dots, \lambda_g \geq 0$. Then, for some numerical constant $C > 0$, the group subset estimator (3.2) with $q = 1$ satisfies

$$\begin{aligned} \frac{1}{n} \|\mathbf{f}^0 - \hat{\mathbf{f}}\|_2^2 \leq & \min_{\substack{\boldsymbol{\beta} \in \mathbb{R}^p, \bar{\boldsymbol{\nu}} \in \mathcal{V}(s) \\ \boldsymbol{\beta} = \sum_{k=1}^g \boldsymbol{\nu}^{(k)}}} \frac{1 + \alpha}{(1 - \alpha)n} \|\mathbf{f}^0 - \mathbf{X}\boldsymbol{\beta}\|_2^2 \\ & + \frac{C\sigma^2}{\alpha(1 - \alpha)n} \left[sp_{\max} + s \log\left(\frac{g}{s}\right) + \log(\delta^{-1}) \right] + \frac{C\lambda_{\max}^2}{\alpha(1 - \alpha)\phi(2s)^2} \end{aligned} \quad (3.5)$$

with probability at least $1 - \delta$.

Theorem 3.3 establishes that the shrinkage estimator achieves the bound of the regular estimator up to an additional term that depends on λ_{\max} and $\phi(2s)$. By setting the shrinkage parameters to zero, the dependence on these terms vanishes, and the bounds are identical.

Theorems 3.2 and 3.3 together show that group subset with shrinkage does no worse than group lasso or group subset. This property is helpful because group lasso tends to outperform when the noise is high or the sample size is small, while group subset tends to outperform in the opposite situation. This empirical observation is consistent with the above bounds since the slow rate (3.4) depends on σ/\sqrt{n} while the fast rate (3.5) depends on σ^2/n . Hence, (3.4) is typically the tighter of the two bounds for large σ or small n .

4 Simulations

This section investigates the computational and statistical performance of the proposed estimators on synthetic data. They are compared against group lasso and group versions of SCAD (Fan and Li 2001) and MCP (Zhang 2010). The range of tuning parameters for each estimator is as follows.

- Group subset: a grid of λ_0 chosen adaptively using the method of Proposition 2.2, where the first λ_0 sets all coefficients to zero.
- Group subset+lasso ($q = 1$): a grid of λ_1 containing logarithmically spaced points between λ_1^{\max} and $\lambda_1^{\min} = 10^{-4}\lambda_1^{\max}$, where λ_1^{\max} is the smallest value that sets all coefficients to zero; and for each value of λ_1 , a grid of λ_0 chosen as above.
- Group subset+ridge ($q = 2$): a grid of λ_2 containing logarithmically spaced points between $\lambda_2^{\max} = 100$ and $\lambda_2^{\min} = 10^{-4}$; and for each value of λ_2 , a grid of λ_0 chosen as above.
- Group lasso: a grid of λ containing logarithmically spaced points between λ^{\max} and $\lambda^{\min} = 10^{-4}\lambda^{\max}$, where λ^{\max} is the smallest value that sets all coefficients to zero.
- Group SCAD: the same grid of λ as above; and for each value of λ , a grid of the nonconvexity parameter γ containing logarithmically spaced points between $\gamma^{\max} = 100$ and $\gamma^{\min} = 2 + 10^{-4}$.
- Group MCP: the same grid of λ as above; and for each value of λ , a grid of the nonconvexity parameter γ containing logarithmically spaced points between $\gamma^{\max} = 100$ and $\gamma^{\min} = 1 + 10^{-4}$.

Grids of 100 points are used for the primary tuning parameters (λ_0, λ) and grids of 10 points for the secondary tuning parameters ($\lambda_1, \lambda_2, \gamma$).

4.1 Computational performance

The algorithms of Section 2 are implemented in `grpse1`. Its efficacy is demonstrated here.

4.1.1 Comparisons against a global optimizer

We begin by evaluating the computational performance of `grpse1` for group subset relative to `Gurobi`, a global optimizer. `Gurobi` is applied to a mixed-integer program representation of

the group subset problem (see Appendix C.1). The aim here is to understand any optimality gaps from `grpssel`. Synthetic datasets are generated according to the regression model

$$y_i = \mathbf{x}_i^\top \boldsymbol{\beta}^0 + \varepsilon_i, \quad i = 1 \dots, n,$$

where $\varepsilon_i \sim \mathcal{N}(0, \sigma^2)$. The predictor matrix $\mathbf{X} \in \mathbb{R}^{n \times p}$ is generated by taking n iid draws from $\mathcal{N}(\mathbf{0}, \boldsymbol{\Sigma})$ and standardizing the columns to have mean zero and unit l_2 -norm. The correlation matrix $\boldsymbol{\Sigma}$ is constructed element-wise as $\Sigma_{i,j} = \rho^{1(i \neq j)}$, where $\rho \in \{0, 0.5, 0.9\}$. This constant correlation structure is chosen to demonstrate algorithmic performance in a worst-case scenario. The noise parameter σ is set to achieve a signal-to-noise ratio (SNR) of 10, where $\text{SNR} := \text{Var}(\mathbf{f}^0)/\sigma^2$ and $\mathbf{f}^0 = \mathbf{X}\boldsymbol{\beta}^0$ here. The number of observations $n = 500$ and number of predictors $p = 1,000$. The predictors are divided into 200 evenly-sized groups and five groups have nonzero coefficients: $\beta_1^0 = \dots = \beta_5^0 = 1$. We record the optimality gap (square loss relative to that of `Gurobi` as evaluated at the true sparsity level) and the run time. `Gurobi` is set with a time limit of 1200 seconds on 32 cores of an AMD Ryzen Threadripper 3970X.

The metrics are aggregated over 10 independent simulations and reported in Table 4.1. Averages are reported with standard errors in parentheses. In the uncorrelated scenario

	Optimality gap	Run time (secs.)
$\rho = 0$		
<code>grpssel</code> (cd)	0.00% (0.00%)	0.20 (0.00)
<code>grpssel</code> (cd+ls)	0.00% (0.00%)	1.16 (0.12)
<code>Gurobi</code>	0.00% (0.00%)	49.85 (6.72)
$\rho = 0.5$		
<code>grpssel</code> (cd)	10.18% (1.70%)	0.75 (0.02)
<code>grpssel</code> (cd+ls)	1.52% (0.54%)	1.58 (0.04)
<code>Gurobi</code>	0.00% (0.00%)	>1200 (0.00)
$\rho = 0.9$		
<code>grpssel</code> (cd)	2.68% (0.42%)	2.04 (0.05)
<code>grpssel</code> (cd+ls)	0.19% (0.09%)	2.96 (0.07)
<code>Gurobi</code>	0.00% (0.00%)	>1200 (0.00)

Table 4.1: Comparisons of algorithms for the group subset estimator. Metrics are aggregated over 10 synthetic datasets generated with $\text{SNR} = 10$, $n = 500$, $p = 1,000$, $g = 200$, and $p_1 = \dots = p_g = 5$. Averages are reported next to (one) standard errors in parentheses. Abbreviation “cd” is coordinate descent and “cd+ls” is coordinate descent with local search.

($\rho = 0$), all three algorithms are equally effective at optimization. In the moderate- ($\rho = 0.5$) and high-correlation ($\rho = 0.9$) scenarios, local search proves its worth, nearly eliminating any gap between `grpssel` and `Gurobi`. `Gurobi` remains the gold standard in the higher correlation scenarios, though it does not terminate in the allocated time. Nevertheless, `grpssel` can deliver solutions nearly as good as those from `Gurobi` in a fraction of the time. Moreover, the times quoted for `grpssel` correspond to an entire regularization path of 100 solutions versus a single point on the path for `Gurobi`. When the additional burden of cross-validating the tuning parameters is factored in, the run times from `Gurobi` can become prohibitive.

4.1.2 Comparisons against an existing implementation

We now compare the computational performance of `grpsel` against `grpreg` (Breheny and Huang 2015), a popular implementation for group lasso, group SCAD, and group MCP. These estimators each solve different optimization problems, so it does not make sense to ask whether one implementation is faster than another for the same problem. Rather, the purpose of these comparisons is to provide indications of run time and computational complexity for alternative approaches to group selection. Both `grpsel` and `grpreg` are set with a convergence tolerance of 10^{-4} . All run times and iteration counts are measured with reference to the coordinate descent algorithms of each package over a grid of the primary tuning parameter. Where there is a secondary tuning parameter, the figures reported are averaged over the secondary parameter, e.g., the total time taken to evaluate a 100×10 grid of parameters divided by 10.

The results as aggregated over 10 synthetic datasets are reported in Figure 4.1. The vertical bars are averages and the error bars are standard errors. For $p = 1,000$ and

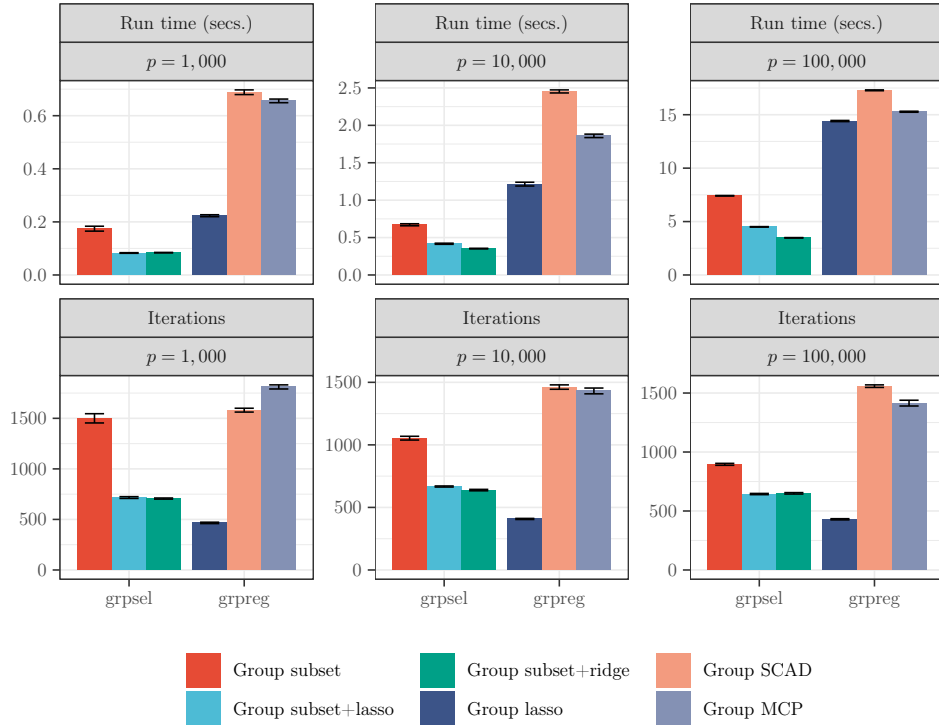


Figure 4.1: Comparisons of packages and estimators for group selection. Metrics are aggregated over 10 synthetic datasets generated with $\text{SNR} = 10$, $\rho = 0$, $n = 500$, $g = p/5$, and $p_1 = \dots = p_g = 5$. Vertical bars represent averages and error bars denote (one) standard errors.

$p = 10,000$, `grpsel` can compute an entire regularization path in less than a second. Group subset+lasso and group subset+ridge yield the lowest times overall, requiring fewer iterations to converge thanks to shrinkage. For $p = 100,000$, `grpsel` still takes less than 10 seconds

to fit a path. `grpreg` is also impressive in this scenario, though relative to `grpsel` it is slower. Group lasso converges in the fewest iterations, closely followed by group subset+ridge and group subset+lasso. Group MCP and group SCAD always take more than a thousand iterations to converge.

4.2 Statistical performance

We now study the comparative finite-sample properties of the group estimators in fitting sparse semiparametric models. Recall $E[y] = \sum_j f_j(x_j)$, and f_j can be zero, linear, or nonlinear. We follow the approach of Chouldechova and Hastie (2015) in using overlapping groups and regression splines. Briefly, for every x_j , an orthogonal spline is computed and two groups are formed: a linear group containing the first term of the spline (assumed equal to x_j) and a nonlinear group containing all terms of the spline. Due to the linear and nonlinear groups overlapping, the fit \hat{f}_j is nonlinear whenever the nonlinear group is selected regardless of whether the linear group is also selected. The group penalty parameters are scaled to control the trade-off between fitting f_j as linear or nonlinear. For group subset or group lasso penalty parameter λ , we set $\lambda_k = \alpha\lambda$ for k a linear group and $\lambda_k = (1 - \alpha)\lambda$ for k a nonlinear group. The scalar α is cross-validated over the grid $\{0.25, 0.30, \dots, 0.50\}$. Taking group subset as an example, when $\alpha = 0.25$, a nonlinear group incurs three times the penalization of a linear group so that it is strongly preferable for x_j to enter the model linearly. When $\alpha = 0.50$, the penalization is equal, and x_j always enters the model nonlinearly.

4.2.1 Setup

Synthetic datasets are generated according to the regression model

$$y_i = f^0(\mathbf{x}_i^*) + \varepsilon_i, \quad i = 1, \dots, n,$$

where $f^0(\mathbf{x}_i^*) = \sum_j f_j^0(x_{ij}^*)$ and $\varepsilon_i \sim \mathcal{N}(0, \sigma^2)$. The matrix $\mathbf{X}^* = (\mathbf{x}_1^*, \dots, \mathbf{x}_n^*)^\top \in \mathbb{R}^{n \times 1000}$ is treated as fixed and constructed as follows. First, n iid observations are drawn from $\mathcal{N}(\mathbf{0}, \mathbf{\Sigma})$, where $\mathbf{\Sigma}$ is Toeplitz with elements $\Sigma_{i,j} = \rho^{|i-j|}$ and $\rho \in \{0.5, 0.9\}$. The standard normal distribution function is applied to each column of this sample to produce uniformly distributed variables that conform to $\mathbf{\Sigma}$ (see Falk 1999). Finally, each column is min-max scaled to the interval $[-1, 1]$. Ten columns are selected at random to construct the response: six using the linear function $f(x) = x$, two using $f(x) = \cos(\pi x)$, and two using $f(x) = \sin(\pi x)$. The remaining columns are unassociated with the response, i.e., $f(x) = 0$ for these. All functions evaluations are scaled to mean zero and variance one. The noise parameter σ is chosen to attain SNR = 1. We take n between 100 and 1000 over a grid of seven values equispaced on the log scale.

The matrix \mathbf{X} is formed by expanding each column of \mathbf{X}^* using a cubic thin-plate spline containing three knots at equispaced quantiles.⁵ Four terms are in each spline so that $p = 4,000$. The number of groups $g = 2,000$.

As a measure of loss, we report estimation error relative to the null model:

$$\text{Relative estimation error} := \frac{\|\mathbf{f}^0 - \hat{\mathbf{f}}\|_2^2}{\|\mathbf{f}^0\|_2^2}.$$

⁵The splines are computed using the `basis_tps` function of the R package `npreg`.

The best possible relative estimation error is zero and the null value is one. In addition, we report the number of fitted functions that are nonzero. As a measure of support recovery, we report the micro F1-score for the classification of linear and nonlinear functions:

$$\text{F1-score} := \frac{2 \cdot \text{True positives}}{2 \cdot \text{True positives} + \text{False positives} + \text{False negatives}}.$$

The best possible F1-score is zero and the null value is one. These metrics are all evaluated with respect to tuning parameters that minimize five-fold cross-validation error. Coordinate descent with local search is used to compute the group subset estimators.

4.2.2 Results

The metrics under consideration are aggregated over 10 simulations and reported in Figure 4.2. The first column of plots pertains to $\rho = 0.5$, the moderate configuration of the correlation parameter—the more challenging configuration where $\rho = 0.9$ relates to the second column. The solid lines are averages and the error bars are standard errors.

Consider first the three group subset estimators. Group subset exhibits excellent performance for large n but fares relatively poorly in smaller sample sizes, roughly when $n < 400$ in the moderate-correlation scenario and later when $n < 500$ in the high-correlation scenario. Thanks to their shrinkage effect, group lasso and ridge penalization improve the performance of group subset considerably in smaller samples. As n increases, group subset+lasso and group subset+ridge lower the degree of shrinkage, eventually behaving like group subset. In contrast to group subset, the shrinkage estimators start with fairly dense models for small n and move towards sparser models as n increases.

Group lasso behaves contrarily to group subset, performing relatively capably for small n but poorly for large n . In addition, it has the unappealing property of failing to converge to the correct sparsity level, leading to mediocre F1-scores. Group SCAD and group MCP try to correct this behavior via their nonconvexity parameters by tapering off the degree of shrinkage. Group MCP is more successful in its attempts than group SCAD. Even so, there remains a gap between group MCP and the group subset estimators. The latter converge earlier to the right sparsity level and the correct model. The gap is most stark in the high-correlation scenario.

Appendix C.2 presents classification results. The findings are broadly consistent with those above.

5 Data analyses

This section studies two contemporary problems: modeling foot traffic in major supermarkets and modeling recessions in the business cycle. Both problems are characterized by the availability of many candidate predictors and the possibility for misspecification of linear models. These characteristics motivate consideration of sparse semiparametric models.

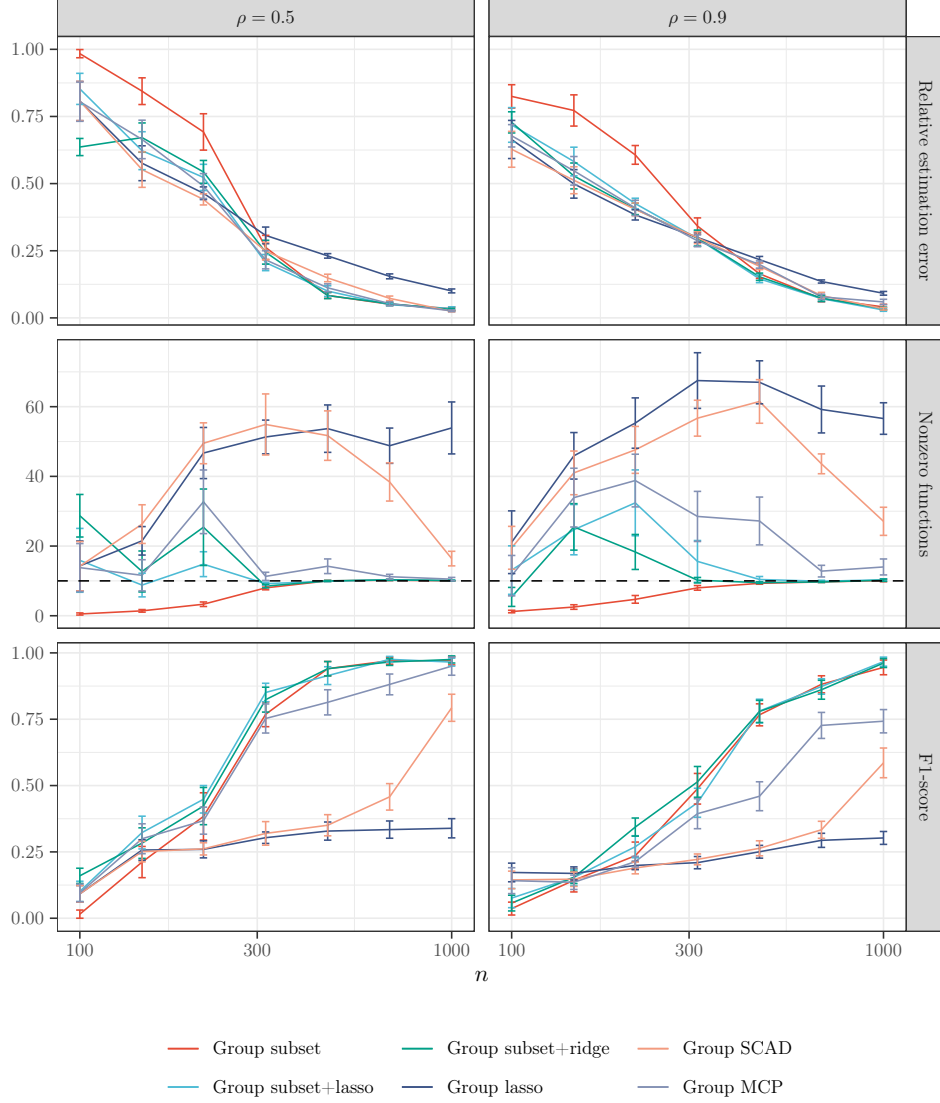


Figure 4.2: Comparisons of estimators for sparse semiparametric regression. Metrics are aggregated over 10 synthetic datasets generated with $\text{SNR} = 1$, $p = 4,000$, and $g = 2,000$. Solid lines represent averages and error bars denote (one) standard errors. Dashed lines indicate the true number of nonzero functions.

5.1 Supermarket foot traffic

The first dataset contains anonymized data on foot traffic and sales volumes for a major Chinese supermarket (see Wang 2009).⁶ The task is to model foot traffic using the sales volumes of different products. To facilitate managerial decision-making, the fitted model should identify a subset of products that well-predict foot traffic (i.e., it should be sparse).

The sample contains $n = 464$ days. We randomly hold out 10% of the data as a testing set and use the remaining data as a training set. Sales volumes are available for 6,398 products. A four-term thin-plate spline is used for each product, resulting in $p = 25,592$ predictors and $g = 12,796$ groups. As a measure of predictive accuracy, we report the out-of-sample mean square error:

$$\text{Mean square error} := \frac{1}{|\mathcal{T}|} \sum_{i \in \mathcal{T}} (y_i - \hat{y}_i)^2,$$

where \mathcal{T} indexes observations in the testing set and \hat{y}_i is a prediction of y_i . We also report the number of fitted functions that are nonzero. As benchmarks, we include random forest and lasso, which respectively produce dense nonparametric models and sparse linear models. In addition, the (unconditional) mean is evaluated as a predictive method to assess the value added by the predictors. Five-fold cross-validation is used to choose tuning parameters. The group subset estimators are computed using coordinate descent (without local search).

The metrics under consideration are aggregated over 10 training-testing set splits and reported in Table 5.1. Averages are reported with standard errors in parentheses. The group

	Mean square error	Nonzero functions		
		Total	Linear	Nonlinear
Group subset+lasso	0.073 (0.007)	157.5 (5.4)	97.2 (11.0)	60.3 (7.5)
Group subset+ridge	0.069 (0.009)	230.1 (8.7)	188.9 (11.4)	41.2 (3.5)
Group lasso	0.074 (0.007)	268.0 (25.2)	63.0 (30.6)	205.0 (18.1)
Group MCP	0.074 (0.007)	199.1 (6.7)	46.1 (20.2)	153.0 (19.9)
Lasso	0.077 (0.010)	163.2 (6.9)	163.2 (6.9)	-
Random forest	0.138 (0.015)	-	-	-
Mean	1.018 (0.047)	-	-	-

Table 5.1: Comparisons of methods for modeling supermarket foot traffic. Metrics are aggregated over 10 splits of the data into training and testing sets. Averages are reported next to (one) standard errors in parentheses.

estimators used to fit sparse semiparametric models all lead to lower mean square error than other methods. Group subset+ridge yields the best predictions, followed by group subset+lasso. The latter estimator has the edge of selecting the fewest products among the sparse methods on average. Lasso yields models that are nearly as sparse but at the same time are also less predictive, signifying linearity might be too restrictive. Random forest is markedly worse than any sparse method. It appears only a small fraction of products explain foot traffic, around 2–3%.

⁶Available at www.personal.psu.edu/ril4/DataScience/index.html.

5.2 Economic recessions

The second dataset contains monthly data on macroeconomic series for the United States (see McCracken and Ng 2016).⁷ The dataset is augmented with the National Bureau of Economic Research recession indicator, a dummy variable that indicates whether a given month is a period of recession or expansion.⁸ The task is to model the recession indicator using the macroeconomic series. Such models are useful for scenario analysis and for assessing economic conditions in the absence of low-frequency variables such as quarterly GDP growth.

The sample contains $n = 739$ months, ending in September 2020. It includes the COVID-19 recession. We again randomly hold out 10% of the data as a testing set and use the remaining data as a training set. Because there are relatively few recessionary periods, a stratified split is applied so that the proportion of recessions in the testing and training sets are equal. The dataset has 128 macroeconomic series. Applying a four-term thin-plate spline to each series yields $p = 512$ predictors and $g = 256$ groups. To evaluate predictive accuracy, we report the out-of-sample mean logistic loss:

$$\text{Mean logistic loss} := \frac{1}{|\mathcal{T}|} \sum_{i \in \mathcal{T}} (-y_i \log(\hat{y}_i) - (1 - y_i) \log(1 - \hat{y}_i)).$$

The remaining metrics and methods are as before. The group subset estimators are computed using coordinate descent with local search.

The results as aggregated over 10 training-testing set splits are reported in Table 5.2. Sparse semiparametric models predict recessionary periods well. Group subset+ridge is again

	Mean logistic loss	Nonzero functions		
		Total	Linear	Nonlinear
Group subset+lasso	0.153 (0.020)	31.4 (2.9)	16.0 (2.2)	15.4 (2.6)
Group subset+ridge	0.145 (0.020)	73.0 (6.9)	1.2 (0.7)	71.8 (7.5)
Group lasso	0.168 (0.023)	38.6 (1.5)	19.9 (2.1)	18.7 (2.5)
Group MCP	0.178 (0.020)	28.3 (0.8)	13.4 (1.6)	14.9 (1.9)
Lasso	0.186 (0.023)	29.4 (1.2)	29.4 (1.2)	-
Random forest	0.153 (0.009)	-	-	-
Mean	0.399 (0.000)	-	-	-

Table 5.2: Comparisons of methods for modeling economic recessions. Metrics are aggregated over 10 splits of the data into training and testing sets. Averages are reported next to (one) standard errors in parentheses.

best, while lasso is worst, highlighting the value in allowing for nonlinearity. Compared with the other estimators, group subset+ridge delivers almost entirely nonlinear models. Its models are also denser on average. On the other hand, group subset+lasso, group lasso, and group MCP use an even split between linear and nonlinear functions. Group subset+lasso yields the lowest loss among these three, and it may be preferable to group subset+ridge

⁷The December 2020 vintage is used, available at <https://research.stlouisfed.org/econ/mccracken/fred-databases/>. See Appendix D.1 for preprocessing steps.

⁸Available at <https://fred.stlouisfed.org/series/USREC>.

if interpretability is sought. All methods improve on the mean, illustrating the predictive content of monthly series.

Unlike the products in the supermarket dataset, the identifiers of the macroeconomic series are available, allowing us to inspect the selected series. In the interest of space, we focus on a subset of six series used in McCracken et al. (2021) as determinants of recessions. For this subset, the type of function fit by each estimator as applied to all $n = 739$ observations is reported in Table 5.3. A checkmark indicates the series entered the model linearly, while a checked box indicates it entered nonlinearly. Except for lasso, T10YFFM (10-year treasury rate

	CMRMTSPLx	FEDFUNDS	INDPRO	PAYEMS	T10YFFM	W875RX1
Group subset+lasso		☑		☑	☑	☑
Group subset+ridge	☑	☑	☑	☑	☑	☑
Group lasso		☑		✓	☑	
Group MCP	☑	☑			☑	
Lasso		✓				

Table 5.3: Estimated function type for select macroeconomic series. Checkmarks indicate a linear fit and checked boxes indicate a nonlinear fit.

minus federal funds rate) and FEDFUNDS (federal funds rate) are treated nonlinearly by every estimator. PAYEMS (nonfarm employment) is fit linear by some and nonlinear by others. The group subset estimators are the only ones to select W875RX1 (real personal income excluding transfers), both of which use a nonlinear fit. Group subset+ridge is the only estimator to select all six series, including CMRMTSPLx (manufacturing and trade sales) and INDPRO (industrial production). Lasso selects only a single series, suggesting it might be unable to approximate the nonlinear effects adequately.

6 Concluding remarks

Despite a broad array of applications, subset selection for grouped predictors is not well-studied, especially in high dimensions where it has remained computationally illusive. This paper represents an effort to close the gap in the general setting of overlapping groups. Our optimization framework consists of low complexity algorithms that come with convergence results. A theoretical analysis of the proposed estimators illuminates some of their finite-sample properties. They estimators behave favorably in simulation, exhibiting excellent support recovery when fitting sparse semiparametric models. In real-world modeling tasks, they improve on popular benchmarks.

Our implementation `grpse1` is available on the R repository CRAN.

Acknowledgments

Ryan Thompson’s research was supported by an Australian Government Research Training Program (RTP) Scholarship.

References

- Beck, A. (2017). *First-order methods in optimization*. MOS-SIAM Series on Optimization. Philadelphia, PA, USA: Society for Industrial and Applied Mathematics and Mathematical Optimization Society.
- Beck, A. and Eldar, Y. C. (2013). “Sparsity constrained nonlinear optimization: Optimality conditions and algorithms”. *SIAM Journal on Optimization* 23.3, pp. 1480–1509.
- Beck, A. and Tetruashvili, L. (2013). “On the convergence of block coordinate descent type methods”. *SIAM Journal on Optimization* 23.4, pp. 2037–2060.
- Bertsimas, D. and King, A. (2016). “OR Forum—An algorithmic approach to linear regression”. *Operations Research* 64.1, pp. 2–16.
- Breheny, P. and Huang, J. (2011). “Coordinate descent algorithms for nonconvex penalized regression, with applications to biological feature selection”. *Annals of Applied Statistics* 5.1, pp. 232–253.
- (2015). “Group descent algorithms for nonconvex penalized linear and logistic regression models with grouped predictors”. *Statistics and Computing* 25.2, pp. 173–187.
- Breiman, L. (1996). “Heuristics of instability and stabilization in model selection”. *Annals of Statistics* 24.6, pp. 2350–2383.
- Breitung, J. and Eickmeier, S. (2011). “Testing for structural breaks in dynamic factor models”. *Journal of Econometrics* 163.1, pp. 71–84.
- Chouldechova, A. and Hastie, T. (2015). “Generalized additive model selection”. Preprint. arXiv: [1506.03850](#).
- De Mol, C., Giannone, D., and Reichlin, L. (2008). “Forecasting using a large number of predictors: Is Bayesian shrinkage a valid alternative to principal components?” *Journal of Econometrics* 146.2, pp. 318–328.
- Dedieu, A., Hazimeh, H., and Mazumder, R. (2020). “Learning sparse classifiers: Continuous and mixed integer optimization perspectives”. Preprint. arXiv: [2001.06471](#).
- Falk, M. (1999). “A simple approach to the generation of uniformly distributed random variables with prescribed correlations”. *Communications in Statistics - Simulation and Computation* 28.3, pp. 785–791.
- Fan, J., Guo, Y., and Zhu, Z. (2020). “When is best subset selection the “best”?” Preprint. arXiv: [2007.01478](#).
- Fan, J. and Li, R. (2001). “Variable selection via nonconcave penalized likelihood and its oracle properties”. *Journal of the American Statistical Association* 96.456, pp. 1348–1360.
- Friedman, J., Hastie, T., Höfling, H., and Tibshirani, R. (2007). “Pathwise coordinate optimization”. *Annals of Applied Statistics* 1.2, pp. 302–332.
- Guo, Y., Berman, M., and Gao, J. (2014). “Group subset selection for linear regression”. *Computational Statistics and Data Analysis* 75, pp. 39–52.
- Hastie, T., Tibshirani, R., and Tibshirani, R. (2020). “Best subset, forward stepwise or lasso? Analysis and recommendations based on extensive comparisons”. *Statistical Science* 35.4, pp. 579–592.
- Hastie, T., Tibshirani, R., and Wainwright, M. (2015). *Statistical learning with sparsity*. Chapman & Hall/CRC Monographs on Statistics and Applied Probability. Boca Raton, FL, USA: CRC Press.

- Hazimeh, H. and Mazumder, R. (2020). “Fast best subset selection: Coordinate descent and local combinatorial optimization algorithms”. *Operations Research* 68.5, pp. 1517–1537.
- Hazimeh, H., Mazumder, R., and Radchenko, P. (2021). “Grouped variable selection with discrete optimization: Computational and statistical perspectives”. Preprint. arXiv: [2104.07084](#).
- Hoerl, A. E. and Kennard, R. W. (1970). “Ridge regression: Biased estimation for nonorthogonal problems”. *Technometrics* 12.1, pp. 55–67.
- Jacob, L., Obozinski, G., and Vert, J.-P. (2009). “Group lasso with overlap and graph lasso”. *Proceedings of the 26th International Conference on Machine Learning*, pp. 433–440.
- Laurent, B. and Massart, P. (2000). “Adaptive estimation of a quadratic functional by model selection”. *Annals of Statistics* 28.5, pp. 1302–1338.
- Li, J. and Chen, W. (2014). “Forecasting macroeconomic time series: Lasso-based approaches and their forecast combinations with dynamic factor models”. *International Journal of Forecasting* 30.4, pp. 996–1015.
- Lim, M. and Hastie, T. (2015). “Learning interactions via hierarchical group-lasso regularization”. *Journal of Computational and Graphical Statistics* 24.3, pp. 627–654.
- Lou, Y., Bien, J., Caruana, R., and Gehrke, J. (2016). “Sparse partially linear additive models”. *Journal of Computational and Graphical Statistics* 25.4, pp. 1026–1040.
- Lounici, K., Pontil, M., van de Geer, S., and Tsybakov, A. B. (2011). “Oracle inequalities and optimal inference under group sparsity”. *Annals of Statistics* 39.4, pp. 2164–2204.
- Mazumder, R., Radchenko, P., and Dedieu, A. (2020). “Subset selection with shrinkage: Sparse linear modeling when the SNR is low”. Preprint. arXiv: [1708.03288](#).
- McCracken, M. W., McGillicuddy, J. T., and Owyang, M. T. (2021). “Binary conditional forecasts”. *Journal of Business and Economic Statistics*, In press.
- McCracken, M. W. and Ng, S. (2016). “FRED-MD: A monthly database for macroeconomic research”. *Journal of Business and Economic Statistics* 34.4, pp. 574–589.
- Meier, L., van de Geer, S., and Bühlmann, P. (2008). “The group lasso for logistic regression”. *Journal of the Royal Statistical Society: Series B (Statistical Methodology)* 70.1, pp. 53–71.
- Obozinski, G., Jacob, L., and Vert, J.-P. (2011). “Group lasso with overlaps: The latent group lasso approach”. Preprint. arXiv: [1110.0413](#).
- Obozinski, G., Taskar, B., and Jordan, M. (2006). *Multi-task feature selection*. Tech. rep. URL: <http://citeseerx.ist.psu.edu/viewdoc/download?doi=10.1.1.94.951&rep=rep1&type=pdf>.
- Percival, D. (2012). “Theoretical properties of the overlapping groups lasso”. *Electronic Journal of Statistics* 6, pp. 269–288.
- Raskutti, G., Wainwright, M. J., and Yu, B. (2011). “Minimax rates of estimation for high-dimensional linear regression over ℓ_q -balls”. *IEEE Transactions on Information Theory* 57.10, pp. 6976–6994.
- Ravikumar, P., Lafferty, J., Liu, H., and Wasserman, L. (2009). “Sparse additive models”. *Journal of the Royal Statistical Society: Series B (Statistical Methodology)* 71.5, pp. 1009–1030.
- Rigollet, P. (2015). *18.S997: High dimensional statistics. Lecture notes*.
- Simon, N. and Tibshirani, R. (2012). “Standardization and the group lasso penalty”. *Statistica Sinica* 22.3, pp. 983–1001.

- Tibshirani, R. (1996). “Regression shrinkage and selection via the lasso”. *Journal of the Royal Statistical Society: Series B (Methodological)* 58.1, pp. 267–288.
- Tseng, P. (2001). “Convergence of a block coordinate descent method for nondifferentiable minimization”. *Journal of Optimization Theory and Applications* 109.3, pp. 475–494.
- Wang, H. (2009). “Forward regression for ultra-high dimensional variable screening”. *Journal of the American Statistical Association* 104.488, pp. 1512–1524.
- Yuan, M. and Lin, Y. (2006). “Model selection and estimation in regression with grouped variables”. *Journal of the Royal Statistical Society: Series B (Statistical Methodology)* 68.1, pp. 49–67.
- Zhang, C.-H. (2010). “Nearly unbiased variable selection under minimax concave penalty”. *Annals of Statistics* 38.2, pp. 894–942.
- Zhang, Y., Zhu, J., Zhu, J., and Wang, X. (2021). “Certifiably polynomial algorithm for best group subset selection”. Preprint. arXiv: [2104.12576](https://arxiv.org/abs/2104.12576).

Appendix A Computation

A.1 Proof of Proposition 2.1

Proof. The subscript k is dropped from c_k , λ_{0k} , λ_{1k} , and λ_{2k} to simplify the notation. Since the objective is treated as a function in the k th group of coordinates β_k only, we have

$$\begin{aligned}\bar{F}_c(\beta; \tilde{\beta}) &\propto \nabla_k L(\tilde{\beta})^\top (\beta_k - \tilde{\beta}_k) + \frac{c}{2} \|\beta_k - \tilde{\beta}_k\|_2^2 + \lambda_0 1(\|\beta_k\|_2 \neq 0) + \lambda_1 \|\beta_k\|_2 + \lambda_2 \|\beta_k\|_2^2 \\ &\propto \frac{c}{2} \left\| \beta_k - \left(\tilde{\beta}_k - \frac{1}{c} \nabla_k L(\tilde{\beta}) \right) \right\|_2^2 + \lambda_0 1(\|\beta_k\|_2 \neq 0) + \lambda_1 \|\beta_k\|_2 + \lambda_2 \|\beta_k\|_2^2 \\ &= \frac{c + 2\lambda_2}{2} \left\| \beta_k - \frac{c}{c + 2\lambda_2} \hat{\beta}_k \right\|_2^2 + \lambda_0 1(\|\beta_k\|_2 \neq 0) + \lambda_1 \|\beta_k\|_2,\end{aligned}$$

where $\hat{\beta}_k = \tilde{\beta}_k - 1/c \nabla_k L(\tilde{\beta})$. When $\lambda_1 = 0$, it is not hard to see a minimizer of $\bar{F}_c(\beta; \tilde{\beta})$ is

$$\beta_k^* = \begin{cases} \frac{c}{c + 2\lambda_2} \hat{\beta}_k & \text{if } \frac{c}{c + 2\lambda_2} \|\hat{\beta}_k\|_2 \geq \sqrt{\frac{2\lambda_0}{c + 2\lambda_2}} \\ \mathbf{0} & \text{otherwise.} \end{cases} \quad (\text{A.1})$$

When $\lambda_0 = 0$ and $\lambda_1 > 0$ (and hence $\lambda_2 = 0$), the minimizer is

$$\beta_k^* = \begin{cases} \left(1 - \frac{\lambda_1}{c \|\hat{\beta}_k\|_2} \right)_+ \hat{\beta}_k & \text{if } \left(1 - \frac{\lambda_1}{c \|\hat{\beta}_k\|_2} \right)_+ \|\hat{\beta}_k\|_2 \geq 0 \\ \mathbf{0} & \text{otherwise.} \end{cases} \quad (\text{A.2})$$

This expression follows from the proximal operator for the l_2 -norm (Beck 2017). Combining (A.1) with (A.2) leads to the result of the proposition. \square

A.2 Proof of Lemma 2.2

Proof. Denote by β^* the result of applying the thresholding function (2.5) to $\tilde{\beta}$. Starting from the inequality (2.2) with $\beta = \beta^*$, we add $\Omega(\beta^*)$ to both sides to obtain

$$F(\beta^*) \leq L(\tilde{\beta}) + \nabla_k L(\tilde{\beta})^\top (\beta_k^* - \tilde{\beta}_k) + \frac{c_k}{2} \|\beta_k^* - \tilde{\beta}_k\|_2^2 + \Omega(\beta^*),$$

where the left-hand side follows from definition (2.3). Adding $\bar{c}_k/2 \|\beta_k^* - \tilde{\beta}_k\|_2^2$ to both sides and rearranging terms leads to

$$\begin{aligned} F(\beta^*) &\leq L(\tilde{\beta}) + \nabla_k L(\tilde{\beta})^\top (\beta_k^* - \tilde{\beta}_k) + \frac{\bar{c}_k}{2} \|\beta_k^* - \tilde{\beta}_k\|_2^2 + \Omega(\beta^*) + \frac{c_k - \bar{c}_k}{2} \|\beta_k^* - \tilde{\beta}_k\|_2^2 \\ &= \bar{F}_{\bar{c}_k}(\beta^*; \tilde{\beta}) + \frac{c_k - \bar{c}_k}{2} \|\beta_k^* - \tilde{\beta}_k\|_2^2. \end{aligned}$$

Using $\bar{F}_{\bar{c}_k}(\beta^*; \tilde{\beta}) \leq \bar{F}_{\bar{c}_k}(\tilde{\beta}; \tilde{\beta}) = F(\tilde{\beta})$, we reorganize terms to get

$$F(\tilde{\beta}) - F(\beta^*) \geq \frac{\bar{c}_k - c_k}{2} \|\beta_k^* - \tilde{\beta}_k\|_2^2. \quad (\text{A.3})$$

Now, define the vector

$$\eta_k^{(m)} := \begin{cases} (\beta_1^{(m+1)\top}, \dots, \beta_k^{(m+1)\top}, \beta_{k+1}^{(m)\top}, \dots, \beta_g^{(m)\top})^\top & \text{if } k > 0 \\ \beta^{(m)} & \text{otherwise.} \end{cases}$$

Take $\tilde{\beta} = \eta_{k-1}^{(m)}$ and $\beta^* = \eta_k^{(m)}$ and sum both sides of the inequality (A.3) over $1 \leq k \leq g$ to get

$$\sum_{k=1}^g [F(\eta_{k-1}^{(m)}) - F(\eta_k^{(m)})] = F(\eta_0^{(m)}) - F(\eta_g^{(m)}) \geq \sum_{k=1}^g \frac{\bar{c}_k - c_k}{2} \|\beta_k^{(m+1)} - \beta_k^{(m)}\|_2^2.$$

By definition $\eta_0^{(m)} = \beta^{(m)}$ and $\eta_g^{(m)} = \beta^{(m+1)}$, establishing $\{F(\beta^{(m)})\}_{m \in \mathbb{N}}$ is decreasing. Since $F(\beta)$ is bounded below, $\{F(\beta^{(m)})\}_{m \in \mathbb{N}}$ must converge. \square

A.3 Proof of Theorem 2.1

The proof relies on the following lemma that the active set must stabilize in finitely many iterations. The lemma is established by contradiction along the lines of Dedieu et al. (2020, Theorem 1).

Lemma A.1. *Let $\bar{c}_k > c_k$ for all $k = 1, \dots, g$. Then the sequence of iterates $\{\beta^{(m)}\}_{m \in \mathbb{N}}$ stabilizes to a fixed support within a finite number of iterations.*

Proof. Suppose the support does not stabilize in finitely many iterations. Choose an m such that $\text{gs}(\beta^{(m+1)}) \neq \text{gs}(\beta^{(m)})$. Then at least one group was added or removed from the support, i.e., there is a k such that either (1) $\beta_k^{(m)} = \mathbf{0}$ and $\beta_k^{(m+1)} \neq \mathbf{0}$ or (2) $\beta_k^{(m)} \neq \mathbf{0}$ and $\beta_k^{(m+1)} = \mathbf{0}$. Consider case (1). It follows from Lemma 2.2

$$F(\beta^{(m)}) - F(\beta^{(m+1)}) \geq \frac{\bar{c}_k - c_k}{2} \|\beta_k^{(m+1)}\|_2^2,$$

and, because $\beta_k^{(m+1)}$ is the output of the thresholding function (2.5), it holds $\beta_k^{(m+1)} \geq \sqrt{2\lambda_{0k}/(\bar{c}_k + 2\lambda_{2k})}$. These inequalities together imply

$$F(\beta^{(m)}) - F(\beta^{(m+1)}) \geq (\bar{c}_k - c_k) \frac{\lambda_{0k}}{\bar{c}_k + 2\lambda_{2k}}.$$

Similar working yields the same inequality for case (2). For $\bar{c}_k > c_k$, the quantity on the right-hand side is strictly positive. Hence, a change to the support yields a strict decrease in the objective value. However, if the support changes infinitely many times, this contradicts that $F(\beta)$ is bounded below. Thus, the support must stabilize in finitely many iterations. \square

We are now ready to prove Theorem 2.1.

Proof. From Lemma A.1, there exists a finite m^* such that the subsequence of iterates $\{\beta^{(m)}\}_{m \geq m^*}$ share the same active set, say \mathcal{A} . Hence, for all $m \geq m^*$ and $k \in \mathcal{A}$ we have

$$\bar{F}_{\bar{c}_k}(\beta; \beta^{(m)}) \propto \frac{\bar{c}_k + 2\lambda_{2k}}{2} \left\| \beta_k - \frac{\bar{c}_k}{\bar{c}_k + 2\lambda_{2k}} \left(\beta_k^{(m)} - \frac{1}{\bar{c}_k} \nabla_k L(\beta^{(m)}) \right) \right\|_2^2 + \lambda_{1k} \|\beta_k\|_2,$$

i.e., the group subset penalty can be treated as fixed. Denote by $\nabla_{\mathbf{v}}^2 \bar{F}_{\bar{c}_k}(\beta; \beta^{(m)})$ the second directional derivative of $\bar{F}_{\bar{c}_k}(\beta; \beta^{(m)})$ along the vector $\mathbf{v} \in \mathbb{R}^p$. The infimum of the minimal eigenvalue of $\nabla_{\mathbf{v}}^2 \bar{F}_{\bar{c}_k}(\beta; \beta^{(m)})$ over all β_k and \mathbf{v} is $\bar{c}_k + 2\lambda_{2k}$. Since $\bar{c}_k > 0$ and $\lambda_{2k} \geq 0$, $\bar{F}_{\bar{c}_k}(\beta; \beta^{(m)})$ is strictly convex. Furthermore, Lemma 2.2 implies the level set $\{\beta \in \mathbb{R}^p : F(\beta) \leq F(\beta^{(0)})\}$ is bounded when the initialization $\beta^{(0)} \in \mathbb{R}^p$, and hence $\{\beta^{(m)}\}_{m \geq m^*}$ is bounded. These conditions are sufficient to invoke Tseng (2001, Theorem 5.1) and establish $\{\beta^{(m)}\}_{m \geq m^*}$ converges to a stationary point β^* of $\bar{F}_{\bar{c}_k}(\beta; \beta^*)$. We conclude by the equality $\bar{F}_{\bar{c}_k}(\beta^*; \beta^*) = F(\beta^*)$ that β^* is also a stationary point of $F(\beta)$. \square

A.4 Proof of Proposition 2.2

Proof. Under the conditions of Theorem 2.1, Algorithm 1 is guaranteed to converge to a stationary point $\hat{\beta}^{(t)}$ such that for all $k \notin \mathcal{A}^{(t)}$ it holds

$$\frac{\left(\|\nabla_k L(\hat{\beta}^{(t)})\|_2 - \lambda_{1k} \right)_+}{\bar{c}_k + 2\lambda_{2k}} < \sqrt{\frac{2\lambda_{0k}^{(t)}}{\bar{c}_k + 2\lambda_{2k}}} = \sqrt{\frac{2\lambda_0^{(t)} p_k}{\bar{c}_k + 2\lambda_{2k}}}.$$

Then initializing Algorithm 1 with $\hat{\beta}^{(t)}$ and using $\lambda_0 = \lambda_0^{(t+1)}$ such that

$$\lambda_0^{(t+1)} < \max_{k \notin \mathcal{A}^{(t)}} \left(\frac{\left(\|\nabla L(\hat{\beta}^{(t)})\|_2 - \lambda_{1k} \right)_+^2}{2p_k(\bar{c}_k + 2\lambda_{2k})} \right)$$

leads to $\hat{\beta}^{(t+1)} \neq \hat{\beta}^{(t)}$. \square

A.5 Other components

We briefly outline other algorithmic components of `grpse1`. These components are similar to those used in the coordinate descent literature (Friedman et al. 2007; Breheny and Huang 2011; Hazimeh and Mazumder 2020).

A.5.1 Sparse residual updates

While Algorithm 1 is running, the residuals $\mathbf{r}^{(m)} = \mathbf{y} - \mathbf{X}\boldsymbol{\beta}^{(m)}$ are required in the gradient calculations. Instead of recomputing $\mathbf{r}^{(m)}$ during each update, the vector is kept in memory and updated only when $\boldsymbol{\beta}^{(m)}$ changes. When required, the update to $\mathbf{r}^{(m)}$ can be performed in $O(p_k n)$ operations as $\mathbf{r}^{(m)} \leftarrow \mathbf{r}^{(m)} - \mathbf{X}_k(\boldsymbol{\beta}_k^{(m)} - \boldsymbol{\beta}_k^{(m-1)})$.

A.5.2 Gradient screening

Rather than cycling through all g groups in each coordinate descent round, it is convenient to restrict the updates to a smaller set of screened groups. The initialization $\boldsymbol{\beta}^{(0)}$ can be used to compute the group-wise gradients $\{\|\nabla_k L(\boldsymbol{\beta}^{(0)})\|_2 / \sqrt{p_k}\}_{k \notin \mathcal{A}^{(0)}}$ which are already available as a consequence of selecting λ_0 dynamically (see Proposition 2.2). The inactive groups whose gradients are among the top 500 largest are classed as “strong,” in addition to the active set of groups. The remaining groups are classed as “weak.” The coordinate descent updates are restricted to the strong groups until convergence is achieved, at which time a further round over the weak groups is performed. If the solution does not change after this further round, convergence is declared. Otherwise, any weak groups that have become active are shifted to the strong set, and the process is repeated.

Gradient screening is also used in local search. Rather than searching through all inactive groups in the inner loop of Algorithm 2, only the inactive groups whose gradients are among the largest 5% are enumerated.

A.5.3 Gradient ordering

The solutions produced by coordinate descent often benefit from greedily ordering the groups. At the beginning of the algorithm, the groups are sorted according to their gradients. Any groups in $\mathcal{A}^{(0)}$ are placed first. The coordinate descent updates then proceed using this new ordering.

A.5.4 Active set updates

The set of active groups typically stabilizes after several rounds of coordinate descent updates. At this time, several additional rounds are required for the nonzero coefficients to converge. Rather than cycling through the full set (or screened set) of groups, the updates are restricted to the active groups only, usually a small subset. Once convergence is achieved on the active set, a further round is performed over the inactive set to confirm overall convergence.

Appendix B Error bounds

B.1 Proof of Theorem 3.1

The proof requires the following lemma.

Lemma B.1. Let $\delta \in (0, 1]$. Let $\mathbf{X} \in \mathbb{R}^{n \times p}$ be a fixed matrix and $\boldsymbol{\varepsilon} \in \mathbb{R}^n$ be a $\mathcal{N}(\mathbf{0}, \sigma^2 \mathbf{I})$ random vector. Define $\boldsymbol{\theta} := \sum_{k=1}^g \boldsymbol{\nu}^{(k)}$ and the random event

$$A_{\bar{\nu}} := \left\{ |\boldsymbol{\varepsilon}^\top \mathbf{X} \boldsymbol{\theta}| \geq \|\mathbf{X} \boldsymbol{\theta}\|_2 C_1 \sigma \sqrt{sp_{\max} + s \log\left(\frac{g}{s}\right) + \log(\delta^{-1})} \right\}.$$

Then, for some numerical constant $C_1 > 0$, the probability of the union $\cup_{\bar{\nu} \in \mathcal{V}(2s)} A_{\bar{\nu}}$ is at most δ .

Proof. For $\mathcal{A} \subseteq \{1, \dots, g\}$, a set of active groups, denote by $\mathcal{S}_{\mathcal{A}} := \cup_{k \in \mathcal{A}} \mathcal{G}_k$ the set of active predictors. Denote the singular value decomposition of $\mathbf{X}_{\mathcal{A}}$ by $\mathbf{U}_{\mathcal{A}} \mathbf{D}_{\mathcal{A}} \mathbf{V}_{\mathcal{A}}^\top$, where $\mathbf{X}_{\mathcal{A}}$ are the columns of \mathbf{X} indexed by $\mathcal{S}_{\mathcal{A}}$. Define the set of unit vectors $\mathcal{B}_2^r := \{\mathbf{u} \in \mathbb{R}^r : \|\mathbf{u}\|_2 \leq 1\}$, and the set of s group-sparse subsets $\mathcal{P}(s) := \{\mathcal{A} \subseteq \{1, \dots, g\} : |\mathcal{A}| = s\}$. For all $\bar{\nu} \in \mathcal{V}(2s)$ such that $\boldsymbol{\theta} \neq \mathbf{0}$, it holds

$$\frac{|\boldsymbol{\varepsilon}^\top \mathbf{X} \boldsymbol{\theta}|}{\|\mathbf{X} \boldsymbol{\theta}\|_2} = \frac{|\boldsymbol{\varepsilon}^\top \mathbf{U}_{\mathcal{A}} \mathbf{D}_{\mathcal{A}} \mathbf{V}_{\mathcal{A}}^\top \boldsymbol{\theta}_{\mathcal{A}}|}{\|\mathbf{D}_{\mathcal{A}} \mathbf{V}_{\mathcal{A}}^\top \boldsymbol{\theta}_{\mathcal{A}}\|_2} \leq \max_{\mathcal{A} \in \mathcal{P}(2s)} \sup_{\mathbf{u} \in \mathcal{B}_2^{|\mathcal{S}_{\mathcal{A}}|}} |\boldsymbol{\varepsilon}^\top \mathbf{U}_{\mathcal{A}} \mathbf{u}|.$$

For any $t \in \mathbb{R}$, this inequality implies

$$\mathbb{P}\left(\cup_{\bar{\nu} \in \mathcal{V}(2s)} \left\{ |\boldsymbol{\varepsilon}^\top \mathbf{X} \boldsymbol{\theta}| \geq \|\mathbf{X} \boldsymbol{\theta}\|_2 t \right\}\right) \leq \mathbb{P}\left(\max_{\mathcal{A} \in \mathcal{P}(2s)} \sup_{\mathbf{u} \in \mathcal{B}_2^{|\mathcal{S}_{\mathcal{A}}|}} |\boldsymbol{\varepsilon}^\top \mathbf{U}_{\mathcal{A}} \mathbf{u}| \geq t\right).$$

Applying Boole's inequality to the right-hand side yields

$$\mathbb{P}\left(\max_{\mathcal{A} \in \mathcal{P}(2s)} \sup_{\mathbf{u} \in \mathcal{B}_2^{|\mathcal{S}_{\mathcal{A}}|}} |\boldsymbol{\varepsilon}^\top \mathbf{U}_{\mathcal{A}} \mathbf{u}| \geq t\right) \leq \sum_{\mathcal{A} \in \mathcal{P}(2s)} \mathbb{P}\left(\sup_{\mathbf{u} \in \mathcal{B}_2^{|\mathcal{S}_{\mathcal{A}}|}} |\boldsymbol{\varepsilon}^\top \mathbf{U}_{\mathcal{A}} \mathbf{u}| \geq t\right).$$

We bound the supremum over $\mathcal{B}_2^{|\mathcal{S}_{\mathcal{A}}|}$ using an ϵ -net argument. Let $\mathcal{E}^{|\mathcal{S}_{\mathcal{A}}|}$ be an ϵ -net of $\mathcal{B}_2^{|\mathcal{S}_{\mathcal{A}}|}$ with respect to l_2 -norm that satisfies $|\mathcal{E}^{|\mathcal{S}_{\mathcal{A}}|}| \leq (3/\epsilon)^{|\mathcal{S}_{\mathcal{A}}|}$. Such an $\mathcal{E}^{|\mathcal{S}_{\mathcal{A}}|}$ is guaranteed to exist for $\epsilon \in (0, 1)$ (Rigollet 2015, Lemma 1.18). Setting $\epsilon = 1/2$, it holds for any $\mathcal{A} \in \mathcal{P}(2s)$ and any $\mathbf{z} \in \mathcal{E}$

$$\sup_{\mathbf{u} \in \mathcal{B}_2^{|\mathcal{S}_{\mathcal{A}}|}} |\boldsymbol{\varepsilon}^\top \mathbf{U}_{\mathcal{A}} \mathbf{u}| \leq 2 \sup_{\mathbf{z} \in \mathcal{E}^{|\mathcal{S}_{\mathcal{A}}|}} |\boldsymbol{\varepsilon}^\top \mathbf{U}_{\mathcal{A}} \mathbf{z}|.$$

Applying Boole's inequality to this bound yields

$$\sum_{\mathcal{A} \in \mathcal{P}(2s)} \mathbb{P}\left(2 \sup_{\mathbf{z} \in \mathcal{E}^{|\mathcal{S}_{\mathcal{A}}|}} |\boldsymbol{\varepsilon}^\top \mathbf{U}_{\mathcal{A}} \mathbf{z}| \geq t\right) \leq \sum_{\mathcal{A} \in \mathcal{P}(2s)} \sum_{\mathbf{z} \in \mathcal{E}^{|\mathcal{S}_{\mathcal{A}}|}} \mathbb{P}\left(2 |\boldsymbol{\varepsilon}^\top \mathbf{U}_{\mathcal{A}} \mathbf{z}| \geq t\right).$$

The cardinality of $\mathcal{P}(2s)$ satisfies $|\mathcal{P}(2s)| = \binom{g}{2s} \leq \log(eg/(2s))^{2s}$. For any $\mathcal{A} \in \mathcal{P}(2s)$, the cardinality of $\mathcal{E}^{|\mathcal{S}_{\mathcal{A}}|}$ satisfies $|\mathcal{E}^{|\mathcal{S}_{\mathcal{A}}|}| \leq 6^{|\mathcal{S}_{\mathcal{A}}|} \leq 6^{2sp_{\max}}$. Since $\mathbf{U}_{\mathcal{A}}$ is orthonormal and \mathbf{z} has unit length, the random variable $\boldsymbol{\varepsilon}^\top \mathbf{U}_{\mathcal{A}} \mathbf{z} \sim \mathcal{N}(0, \sigma^2)$. Using a standard Gaussian tail bound (Rigollet 2015, Lemma 1.4), we have

$$\mathbb{P}\left(2 |\boldsymbol{\varepsilon}^\top \mathbf{U}_{\mathcal{A}} \mathbf{z}| \geq t\right) \leq 2 \exp\left(-\frac{t^2}{8\sigma^2}\right).$$

It follows from the chain of inequalities above

$$\mathbb{P} \left(\bigcup_{\bar{\nu} \in \mathcal{V}(2s)} \left\{ |\boldsymbol{\varepsilon}^\top \mathbf{X}\boldsymbol{\theta}| \geq \|\mathbf{X}\boldsymbol{\theta}\|_2 t \right\} \right) \leq 2 \exp \left(-\frac{t^2}{8\sigma^2} + 2sp_{\max} \log(6) + 2s \log \left(\frac{eg}{2s} \right) \right).$$

Setting $t \geq \sqrt{8\sigma^2[\log(2) + 2sp_{\max} \log(6) + 2s \log(eg/(2s)) + \log(\delta^{-1})]}$ concludes the proof. \square

We are now ready to prove Theorem 3.1.

Proof. Take any $\bar{\nu} \in \mathcal{V}(s)$ and any $\beta \in \mathbb{R}^p$ such that $\beta = \sum_{k=1}^g \nu^{(k)}$. Optimality of $\hat{\nu}$ and $\hat{\beta} = \sum_{k=1}^g \hat{\nu}^{(k)}$ implies

$$\frac{1}{n} \|\mathbf{y} - \mathbf{X}\hat{\beta}\|_2^2 \leq \frac{1}{n} \|\mathbf{y} - \mathbf{X}\beta\|_2^2,$$

which, after some algebra, leads to

$$\frac{1}{n} \|\mathbf{f}^0 - \mathbf{X}\hat{\beta}\|_2^2 \leq \frac{1}{n} \|\mathbf{f}^0 - \mathbf{X}\beta\|_2^2 + \frac{2}{n} |\boldsymbol{\varepsilon}^\top \mathbf{X}(\hat{\beta} - \beta)|.$$

Observe $\hat{\beta} - \beta = \sum_{k=1}^g (\hat{\nu}^{(k)} - \nu^{(k)})$, with at most $2s$ components of $(\hat{\nu}^{(1)} - \nu^{(1)}), \dots, \hat{\nu}^{(g)} - \nu^{(g)}$ not equal to $\mathbf{0}$. An application of Lemma B.1 thus yields the high-probability upper bound

$$\begin{aligned} \frac{2}{n} |\boldsymbol{\varepsilon}^\top \mathbf{X}(\hat{\beta} - \beta)| &\leq \frac{2}{n} \|\mathbf{X}(\hat{\beta} - \beta)\|_2 C_1 \sigma \sqrt{sp_{\max} + s \log \left(\frac{g}{s} \right) + \log(\delta^{-1})} \\ &\leq \frac{2}{n} \left(\|\mathbf{f}^0 - \mathbf{X}\hat{\beta}\|_2 + \|\mathbf{f}^0 - \mathbf{X}\beta\|_2 \right) C_1 \sigma \sqrt{sp_{\max} + s \log \left(\frac{g}{s} \right) + \log(\delta^{-1})}, \end{aligned}$$

where the last line follows from Minkowski's inequality for l_p -norms. Using Young's inequality ($2ab \leq \alpha a^2 + \alpha^{-1} b^2$ for $\alpha > 0$), the first term on the right-hand side is bounded as

$$\begin{aligned} \frac{2}{n} \|\mathbf{f}^0 - \mathbf{X}\hat{\beta}\|_2 C_1 \sigma \sqrt{sp_{\max} + s \log \left(\frac{g}{s} \right) + \log(\delta^{-1})} \\ \leq \frac{\alpha}{n} \|\mathbf{f}^0 - \mathbf{X}\hat{\beta}\|_2^2 + \frac{C_1^2 \sigma^2}{\alpha n} \left[sp_{\max} + s \log \left(\frac{g}{s} \right) + \log(\delta^{-1}) \right]. \end{aligned}$$

A bound for the second term on the right-hand side follows similarly. Putting the results together and rearranging terms, we arrive at

$$\frac{1}{n} \|\mathbf{f}^0 - \mathbf{X}\hat{\beta}\|_2^2 \leq \frac{1+\alpha}{(1-\alpha)n} \|\mathbf{f}^0 - \mathbf{X}\beta\|_2^2 + \frac{2C_1^2 \sigma^2}{\alpha(1-\alpha)n} \left[sp_{\max} + s \log \left(\frac{g}{s} \right) + \log(\delta^{-1}) \right],$$

holding with probability at least $1 - \delta$ for $\alpha \in (0, 1)$. Taking $C \geq 2C_1^2$ completes the proof. \square

B.2 Proof of Theorem 3.2

The proof requires the following lemma.

Lemma B.2. *Let $\delta \in (0, 1]$. Let $\mathbf{X} \in \mathbb{R}^{n \times p}$ be a fixed matrix and $\boldsymbol{\varepsilon} \in \mathbb{R}^n$ be a $\mathcal{N}(\mathbf{0}, \sigma^2 \mathbf{I})$ random vector. Let γ_k be the maximal eigenvalue of $\mathbf{X}_k^\top \mathbf{X}_k / n$, where \mathbf{X}_k is the submatrix of \mathbf{X} corresponding to group k . Define the random event*

$$A_k = \left\{ \|\mathbf{X}_k^\top \boldsymbol{\varepsilon}\|_2 \geq \sqrt{n\gamma_k} \sigma \sqrt{p_k + 2\sqrt{p_k \log(g) + p_k \log(\delta^{-1})} + 2\log(g) + 2\log(\delta^{-1})} \right\}.$$

Then the probability of the union $\cup_{k=1}^g A_k$ is at most δ .

Proof. Denote the singular value decomposition of \mathbf{X}_k by $\mathbf{U}_k \mathbf{D}_k \mathbf{V}_k^\top$. Using the properties of the operator norm, it holds

$$\|\mathbf{X}_k^\top \boldsymbol{\varepsilon}\|_2 = \|\mathbf{V}_k \mathbf{D}_k \mathbf{U}_k^\top \boldsymbol{\varepsilon}\|_2 \leq \sqrt{n\gamma_k} \|\mathbf{U}_k^\top \boldsymbol{\varepsilon}\|_2.$$

For any $t \in \mathbb{R}$, this inequality implies

$$\mathbb{P} \left(\cup_{k=1}^g \{\|\mathbf{X}_k^\top \boldsymbol{\varepsilon}\|_2 \geq \sqrt{n\gamma_k} t\} \right) \leq \mathbb{P} \left(\cup_{k=1}^g \{\|\mathbf{U}_k^\top \boldsymbol{\varepsilon}\|_2 \geq t\} \right).$$

Applying Boole's inequality to the right-hand side yields

$$\mathbb{P} \left(\cup_{k=1}^g \{\|\mathbf{U}_k^\top \boldsymbol{\varepsilon}\|_2 \geq t\} \right) \leq \sum_{k=1}^g \mathbb{P} \left(\|\mathbf{U}_k^\top \boldsymbol{\varepsilon}\|_2 \geq t \right).$$

Since \mathbf{U}_k is orthonormal, the random variable $\|\mathbf{U}_k^\top \boldsymbol{\varepsilon}\|_2^2 / \sigma^2 \sim \chi^2(p_k)$. Using a standard chi-squared tail bound (Laurent and Massart 2000, Lemma 1), we have for $t = p_k + \sqrt{2p_k x} + 2x$ and $x > 0$

$$\mathbb{P} \left(\|\mathbf{U}_k^\top \boldsymbol{\varepsilon}\|_2 \geq \sigma \sqrt{t} \right) \leq \exp(-x).$$

It follows from the chain of inequalities above

$$\mathbb{P} \left(\cup_{k=1}^g \left\{ \|\mathbf{X}_k^\top \boldsymbol{\varepsilon}\|_2 \geq \sqrt{n\gamma_k} \sigma \sqrt{p_k + \sqrt{2p_k x} + 2x} \right\} \right) \leq \exp(-x + \log(g)).$$

Setting $x \geq \log(g) + \log(\delta^{-1})$ concludes the proof. \square

We are now ready to prove Theorem 3.2.

Proof. For any $\bar{\boldsymbol{\nu}} \in \mathcal{V}(s)$ and any $\boldsymbol{\beta} \in \mathbb{R}^p$ such that $\boldsymbol{\beta} = \sum_{k=1}^g \boldsymbol{\nu}^{(k)}$, we have

$$\frac{1}{n} \|\mathbf{y} - \mathbf{X} \hat{\boldsymbol{\beta}}\|_2^2 + 2 \sum_{k=1}^g \lambda_k \|\hat{\boldsymbol{\nu}}^{(k)}\|_2 \leq \frac{1}{n} \|\mathbf{y} - \mathbf{X} \boldsymbol{\beta}\|_2^2 + 2 \sum_{k=1}^g \lambda_k \|\boldsymbol{\nu}^{(k)}\|_2,$$

which leads to

$$\frac{1}{n} \|\mathbf{f}^0 - \mathbf{X} \hat{\boldsymbol{\beta}}\|_2^2 \leq \frac{1}{n} \|\mathbf{f}^0 - \mathbf{X} \boldsymbol{\beta}\|_2^2 + \frac{2}{n} |\boldsymbol{\varepsilon}^\top \mathbf{X} (\hat{\boldsymbol{\beta}} - \boldsymbol{\beta})| + 2 \sum_{k=1}^g \lambda_k \left(\|\boldsymbol{\nu}^{(k)}\|_2 - \|\hat{\boldsymbol{\nu}}^{(k)}\|_2 \right). \quad (\text{B.1})$$

The Cauchy-Schwarz inequality and Minkowski's inequality are applied in turn to get

$$\frac{2}{n}|\boldsymbol{\varepsilon}^\top \mathbf{X}(\hat{\boldsymbol{\beta}} - \boldsymbol{\beta})| \leq \frac{2}{n} \sum_{k=1}^g \|\mathbf{X}_k^\top \boldsymbol{\varepsilon}\|_2 \|\hat{\boldsymbol{\nu}}^{(k)} - \boldsymbol{\nu}^{(k)}\|_2 \leq \frac{2}{n} \sum_{k=1}^g \|\mathbf{X}_k^\top \boldsymbol{\varepsilon}\|_2 (\|\hat{\boldsymbol{\nu}}^{(k)}\|_2 + \|\boldsymbol{\nu}^{(k)}\|_2).$$

Applying Lemma B.2, and using the assumed lower bound on λ_k , yields

$$\frac{2}{n} \sum_{k=1}^g \|\mathbf{X}_k^\top \boldsymbol{\varepsilon}\|_2 (\|\hat{\boldsymbol{\nu}}^{(k)}\|_2 + \|\boldsymbol{\nu}^{(k)}\|_2) \leq 2 \sum_{k=1}^g \lambda_k (\|\hat{\boldsymbol{\nu}}^{(k)}\|_2 + \|\boldsymbol{\nu}^{(k)}\|_2)$$

with high-probability. Plugging this bound into (B.1), we arrive at

$$\frac{1}{n} \|\mathbf{f}^0 - \mathbf{X}\hat{\boldsymbol{\beta}}\|_2^2 \leq \frac{1}{n} \|\mathbf{f}^0 - \mathbf{X}\boldsymbol{\beta}\|_2^2 + 4 \sum_{k=1}^g \lambda_k \|\boldsymbol{\nu}^{(k)}\|_2,$$

holding with probability at least $1 - \delta$. □

B.3 Proof of Theorem 3.3

Proof. Begin with inequality (B.1). First, we bound the term $2/n|\boldsymbol{\varepsilon}^\top \mathbf{X}(\hat{\boldsymbol{\beta}} - \boldsymbol{\beta})|$. Lemma B.1 gives the high-probability upper bound

$$\begin{aligned} \frac{2}{n}|\boldsymbol{\varepsilon}^\top \mathbf{X}(\hat{\boldsymbol{\beta}} - \boldsymbol{\beta})| &\leq \frac{2}{n} \|\mathbf{X}(\hat{\boldsymbol{\beta}} - \boldsymbol{\beta})\|_2 C_1 \sigma \sqrt{sp_{\max} + s \log\left(\frac{g}{s}\right) + \log(\delta^{-1})} \\ &\leq \frac{2}{n} \left(\|\mathbf{f}^0 - \mathbf{X}\hat{\boldsymbol{\beta}}\|_2 + \|\mathbf{f}^0 - \mathbf{X}\boldsymbol{\beta}\|_2 \right) C_1 \sigma \sqrt{sp_{\max} + s \log\left(\frac{g}{s}\right) + \log(\delta^{-1})}. \end{aligned}$$

Using Young's inequality ($2ab \leq \alpha/2a^2 + 2/\alpha b^2$), the first term on the right-hand side is bounded as

$$\begin{aligned} \frac{2}{n} \|\mathbf{f}^0 - \mathbf{X}\hat{\boldsymbol{\beta}}\|_2 C_1 \sigma \sqrt{sp_{\max} + s \log\left(\frac{g}{s}\right) + \log(\delta^{-1})} \\ \leq \frac{\alpha}{2n} \|\mathbf{f}^0 - \mathbf{X}\hat{\boldsymbol{\beta}}\|_2^2 + \frac{2C_1^2 \sigma^2}{\alpha n} \left[sp_{\max} + s \log\left(\frac{g}{s}\right) + \log(\delta^{-1}) \right]. \end{aligned}$$

The second term on the right-hand side is bounded similarly. Now, we bound the remaining term $2 \sum_{k=1}^g \lambda_k (\|\boldsymbol{\nu}^{(k)}\|_2 - \|\hat{\boldsymbol{\nu}}^{(k)}\|_2)$ in (B.1). Minkowski's inequality and Assumption 3.1 give

$$2 \sum_{k=1}^g \lambda_k (\|\boldsymbol{\nu}^{(k)}\|_2 - \|\hat{\boldsymbol{\nu}}^{(k)}\|_2) \leq 2\lambda_{\max} \sum_{k=1}^g \|\boldsymbol{\nu}^{(k)} - \hat{\boldsymbol{\nu}}^{(k)}\|_2 \leq \frac{2\lambda_{\max}}{\sqrt{n}\phi(2s)} \|\mathbf{X}(\boldsymbol{\beta} - \hat{\boldsymbol{\beta}})\|_2.$$

Using Minkowski's inequality again, we have

$$\frac{2\lambda_{\max}}{\sqrt{n}\phi(2s)} \|\mathbf{X}(\boldsymbol{\beta} - \hat{\boldsymbol{\beta}})\|_2 \leq \frac{2\lambda_{\max}}{\sqrt{n}\phi(2s)} \left(\|\mathbf{f}^0 - \mathbf{X}\hat{\boldsymbol{\beta}}\|_2 + \|\mathbf{f}^0 - \mathbf{X}\boldsymbol{\beta}\|_2 \right).$$

Two applications of Young's inequality yields

$$\frac{2\lambda_{\max}}{\sqrt{n}\phi(2s)} \left(\|\mathbf{f}^0 - \mathbf{X}\hat{\boldsymbol{\beta}}\|_2 + \|\mathbf{f}^0 - \mathbf{X}\boldsymbol{\beta}\|_2 \right) \leq \frac{4\lambda_{\max}^2}{\alpha\phi(2s)^2} + \frac{\alpha}{2n} \|\mathbf{f}^0 - \mathbf{X}\hat{\boldsymbol{\beta}}\|_2^2 + \frac{\alpha}{2n} \|\mathbf{f}^0 - \mathbf{X}\boldsymbol{\beta}\|_2^2.$$

Finally, putting the bounds together and simplifying the resulting expression, we have

$$\begin{aligned} \frac{1}{n} \|\mathbf{f}^0 - \mathbf{X}\hat{\boldsymbol{\beta}}\|_2^2 &\leq \frac{1 + \alpha}{(1 - \alpha)n} \|\mathbf{f}^0 - \mathbf{X}\boldsymbol{\beta}\|_2^2 + \frac{4C_1^2\sigma^2}{\alpha(1 - \alpha)n} \left[sp_{\max} + s \log\left(\frac{g}{s}\right) + \log(\delta^{-1}) \right] \\ &\quad + \frac{4\lambda_{\max}^2}{\alpha(1 - \alpha)\phi(2s)^2}, \end{aligned}$$

holding with probability at least $1 - \delta$ for $\alpha \in (0, 1)$. \square

Appendix C Simulations

C.1 Mixed-integer program

Group subset with shrinkage (1.3) as a mixed-integer program is

$$\min_{\substack{\boldsymbol{\beta} \in \mathbb{R}^p, \mathbf{z} \in \{0,1\}^g \\ (\boldsymbol{\beta}_k, 1 - z_k) : \text{SOS-1} \\ -M \leq \beta_j \leq M}} \sum_{i=1}^n \ell(\mathbf{x}_i^\top \boldsymbol{\beta}, y_i) + \sum_{k=1}^g \lambda_{0k} z_k + \sum_{k=1}^g \lambda_{qk} \|\boldsymbol{\beta}_k\|_2^q,$$

where $(\boldsymbol{\beta}_k, 1 - z_k) : \text{SOS-1}$ is a special ordered set (SOS) constraint of type one and M is an optional upper bound on $\|\boldsymbol{\beta}\|_\infty$. These SOS constraints have the property

$$(\boldsymbol{\beta}_k, 1 - z_k) : \text{SOS-1} \implies \boldsymbol{\beta}_k(1 - z_k) = \mathbf{0},$$

thereby enforcing group sparsity on $\boldsymbol{\beta}$. The bounding constant M assists the solver in terminating quicker. In the experiments, $M = 1.25\|\hat{\boldsymbol{\beta}}\|_\infty$ where $\hat{\boldsymbol{\beta}}$ is the least-squares fit on the true set of groups. When groups overlap, the approach of expanding the predictor matrix as described in Section 2 is applicable.

C.2 Classification results

The response is generated as a Bernoulli variable:

$$P(y_i = 1) = \frac{1}{1 + \exp(-f^0(\mathbf{x}_i^*))}, \quad i = 1, \dots, n.$$

The remainder of the simulation design and evaluation metrics are the same as for regression. Figure C.1 reports the results. Compared with regression, group SCAD now performs better in support recovery, though not as well as the group subset estimators.

Appendix D Data analyses

D.1 Macroeconomic data preprocessing

All series are made stationary using standard transformations given in McCracken and Ng (2016). Some series contain missing observations and outliers, which are also treated as missing. These missing values are imputed using the `na_kalman` function of the R package `imputeTS`. Following Breitung and Eickmeier (2011), an observation x_i is treated as an outlier if $|x_i - Q_2|/(Q_3 - Q_1) > 6$ where Q_1 , Q_2 , and Q_3 are the respective quartiles of the data.

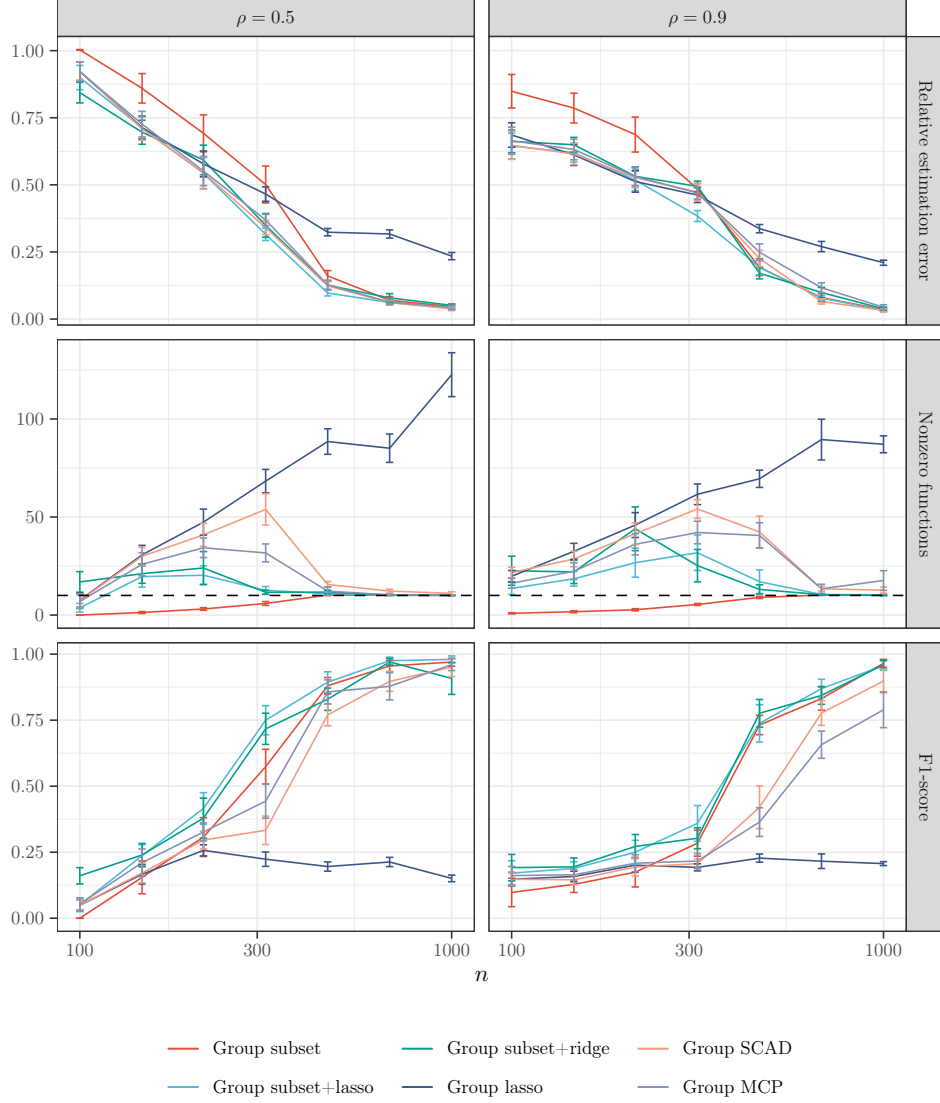


Figure C.1: Comparisons of estimators for sparse semiparametric classification. Metrics are aggregated over 10 synthetic datasets generated with $p = 4,000$ and $g = 2,000$. Solid lines represent averages and error bars denote (one) standard errors. Dashed lines indicate the true number of nonzero functions.